The Ronald O. Perelman Center for Political Science and Economics (PCPSE)
133 South 36th Street
Philadelphia, PA 19104-6297

pier@econ.upenn.edu
http://economics.sas.upenn.edu/pier

PIER Working Paper

24-015

Are We Fragmented Yet? Measuring Geopolitical Fragmentation and Its Causal Effects

JESÚS FERNÁNDEZ-VILLAVERDE
University of Pennsylvania,
NBER, and CEPR

TOMOHIDE MINEYAMA
International Monetary Fund

DONGHO SONG
Johns Hopkins University

June 25, 2024

Are We Fragmented Yet?
Measuring Geopolitical Fragmentation and Its Causal Effects*

Jesús Fernández-Villaverde† Tomohide Mineyama‡ Dongho Song§

University of Pennsylvania, CEPR, NBER International Monetary Fund Johns Hopkins University

June 25, 2024

Abstract

After decades of rising global economic integration, the world economy is now fragmenting. To measure this phenomenon, we introduce an index of geopolitical fragmentation derived from various empirical indicators. This index is developed using a flexible dynamic factor model with time-varying parameters and stochastic volatility. We then employ structural vector autoregressions and local projections to assess the causal effects of changes in fragmentation. Our analysis demonstrates that increased fragmentation negatively impacts the global economy, with emerging economies suffering more than advanced ones. Notably, we document a key asymmetry: fragmentation has an immediate negative effect, while the benefits of reduced fragmentation unfold gradually. A sectoral analysis within OECD economies reveals that industries closely linked to global markets —such as manufacturing, construction, finance, and wholesale and retail trade— are adversely affected. Finally, we examine the interaction between fragmentation and the economic dynamics of regional economic blocs, highlighting significant differences in the impacts across various geopolitical blocs.

JEL Classification: C11, C33, E00, F01, F2, F4, F6

Keywords: Dynamic factor model, causality, geopolitical fragmentation, fragmentation index

*We thank Philip Barrett, Steven Davis, Anna Ilyina, Benjamin Kett, Michele Ruta, and Jonathan Wright for comments on earlier drafts. The views expressed herein are those of the authors and should not be attributed to the IMF, its Executive Board, or its management.

†Fernández-Villaverde: jesusfv@econ.upenn.edu

‡Mineyama: TMineyama@imf.org

§Song: dongho.song@jhu.edu

1 Introduction

Following decades of increasing global economic integration, the world economy shifted course after the 2007-2008 financial crisis. Events such as Brexit and conflicts in the Middle East have strained international relations and prompted policymakers to reconsider their nations' economic strategies. Free trade agreements, once common, have become rare. Instead, large industrial countries frequently announce new tariffs, with the number of trade-restricting measures implemented in 2022 nearly tripling compared to 2019. Consequently, households, firms, and governments are reassessing their operations amid growing geopolitical and trade complexities. For more detailed discussions on this geopolitical fragmentation and its impact on the world economy, see Aiyar et al. (2023a) and Gopinath (2023).

Various indicators reveal discernible trends in this ongoing geopolitical fragmentation: a global slowdown in the flows of goods and capital, increased restrictions on trade and foreign direct investment, heightened political risks, more frequent sanctions and conflicts, tighter capital controls, and growing concerns related to migration. However, no single measure of geopolitical fragmentation fully captures the current state of global economic integration, as each indicator only addresses one aspect of it. Thus, choosing one indicator over another (or an average of them) to study the evolution and implications of geopolitical fragmentation can be arbitrary and may lead to incorrect conclusions or policy recommendations.

Fortunately, dynamic factor models (DFMs) offer a way to create a comprehensive index of geopolitical fragmentation —a numerical measurement of this multifaceted process. The main idea behind a DFM, as pioneered by Sargent and Sims (1977), Geweke (1977), and Stock and Watson (1989), is that many observed indicators of a phenomenon (such as the business cycle or geopolitical fragmentation) are driven by a common unobserved factor. While each indicator is inherently imperfect and contaminated by idiosyncratic noise, we can employ a likelihood-based approach to estimate the unobserved index that captures the underlying dynamics of interest.

The DFM approach has gained popularity in macroeconomics because it is fully data-driven and minimizes the subjective decisions a researcher needs to make. Specifically, we propose a state-of-the-art DFM with time-varying parameters and stochastic volatility. This flexible specification can accommodate missing observations and handle data with different frequencies.

There are two main reasons for estimating such a factor. First, it allows us to gauge the evolution of geopolitical fragmentation. An increase in the factor indicates that the world economy is becoming more fragmented, thus providing a quantitative confirmation (or refutation) of more casual assessments and mitigating the confirmatory bias present in many qualitative evaluations by experts. Second, the estimated factor can be used as an input for other empirical analyses, such as a variable in a structural vector autoregression (SVAR) or

a linear projection (LP) for causality assessment. This enables us to translate changes in the factor (e.g., an increase by 1 standard deviation) into concrete effects on aggregate variables with a sharp economic interpretation (e.g., a 30 basis point reduction in GDP). Our principal aim is to establish an index designed for broad usage, serving the needs of policymakers, practitioners, and academics alike.

After introducing the indicators we employ and discussing our econometric methodology, we present the evolution of our estimated factor. This index reveals three distinct phases. First, there was a period of relative stability in geopolitical fragmentation from 1975 to the early 1990s. Fragmentation then decreased as the collapse of the Soviet Union and market-oriented reforms across many countries led to a spike in globalization. However, following the 2007-2008 financial crisis, geopolitical fragmentation has increased to its highest levels in the sample, with no signs of reversal. Our estimation results align broadly with narrative approaches that have discussed the evolution of geopolitical fragmentation based on qualitative evidence (e.g., Gopinath, 2023).

Next, we use our index as an input for standard causality analysis exercises with SVARs and LPs. Our analysis reveals that a positive one-standard-deviation shock to the fragmentation index (considered adverse) has a detrimental impact on the global economy, with more pronounced negative effects observed in emerging economies compared to advanced economies. The impacts reveal an asymmetry: fragmentation has an immediate negative effect on the global economy, while the positive effects of reduced fragmentation (viewed as an aspect of globalization) unfold with lags. Our findings remain robust under different identification assumptions (e.g., different orderings of variables or a narrative approach) and when considering various control variables, aligning with the approach taken by Caldara and Iacoviello (2022).

To elucidate the economic channels through which fragmentation influences the economy, we scrutinize sectors within OECD economies, chosen primarily due to data availability. The sectoral analysis highlights the adverse effects on industries closely linked to global markets, such as manufacturing, construction, finance, and wholesale and retail trade. Conversely, sectors like agriculture, forestry, fishing, real estate, and public services, which are more insulated from global markets, experience only marginal effects. This sectoral pattern is particularly evident in the case of the U.S. economy.

Finally, we examine the effects of the world economy's fragmentation into increasingly separate geopolitical blocs. We find notable differences in the level of fragmentation among different blocs, such as the U.S.-EU bloc vs. the China-Russia bloc. Fragmentation shocks in the U.S.-EU bloc lead to more pronounced global effects than those in the China-Russia bloc, highlighting the unique characteristics of the latter economic relationship.

Our paper contributes to the expanding literature on geopolitical fragmentation (e.g., Attinasi et al., 2023, Blanga-Gubbay and Rubinova, 2023, Bolhuis et al., 2023, Campos

et al., 2023, Cerdeiro et al., 2021, Clayton et al., 2024, Góes and Bekkers, 2022, Hakobyan et al., 2023, Javorcik et al., 2024, and Utar et al., 2023), building on the summaries provided by Aiyar et al. (2023a) and Gopinath (2023). This literature sheds light on the associated costs, which include the unwinding of gains from globalization, encompassing trade (e.g., Frankel and Romer, 1999; Feenstra, 2006), technology diffusion and adoption (e.g., Bustos, 2011; Acemoglu et al., 2015), cross-border labor and capital flows (e.g., Glennon, 2024; Erten et al., 2021), and international risk sharing (e.g., Obstfeld, 1994). Our paper contributes to this body of work by quantifying the causal effects of fragmentation on aggregate economic variables. While existing papers focus on a single or a few indicators of fragmentation at a time (e.g., Antrás, 2020, Goldberg and Reed, 2023, and Gopinath et al., 2024), this paper addresses that gap by consolidating various aspects.

Geopolitical tensions further contribute to increased uncertainty regarding future policies and the ultimate shape of a fragmented world (e.g., Caldara et al., 2020). The direct costs of trade disruptions include tariffs, inefficiencies from reduced specialization, resource misallocation, diminished economies of scale, and decreased competition (e.g., Melitz and Trefler, 2012). Aiyar et al. (2023a) point out that short-term transition costs stemming from trade disruptions tend to be more pronounced due to the low elasticities of substitution in the short run. In contrast, losses from technological decoupling may materialize over the medium and long term.

Moreover, the impact of these costs may vary across countries. As highlighted by Aiyar et al. (2023a), geoeconomic fragmentation disproportionately affects emerging markets and low-income countries that have the potential for catch-up through trade and financial and technological integration. Gopinath (2023) and Gopinath et al. (2024) add that if disruptions occur primarily between large blocs (e.g., a U.S.-Europe bloc and a China-Russia bloc), some countries, particularly in Latin America or Southeast Asia, may experience gains as "neutral" bystanders.

Given the multiple channels of impact and potential heterogeneity described above, the examination of the cost of fragmentation is an empirical question. The literature has investigated the economic consequences of recent fragmentation episodes, such as Brexit (e.g., Sampson, 2017, and Bloom et al., 2019) and the U.S.-China trade war in 2018-19 (Fajgelbaum and Khandelwal, 2022, review the corresponding literature).

For instance, concerning the 2018 U.S. import tariff hikes, Amiti et al. (2020) report that the increased tariffs are passed through to domestic prices, imposing their direct costs ultimately on consumers. Flaaen and Pierce (2019) and Handley et al. (2020) report negative consequences for U.S. manufacturing employment and exports due to rising import costs and retaliatory tariffs, while Fajgelbaum et al. (2019) find that the aggregate real income loss is modest after accounting for tariff revenues and gains to domestic producers. A few studies (Góes and Bekkers, 2022, Cerdeiro et al., 2021, and Bolhuis et al., 2023) develop general

equilibrium international trade models to estimate the cost of fragmentation. Estimates are substantial but vary widely, ranging from around 1% to 10% of GDP, depending on the scenarios considered and modeling assumptions.

Finally, our paper contributes to the existing body of literature focused on formulating indices or metrics. This includes assessments of uncertainty (e.g., Jurado et al., 2015, and Baker et al., 2016), geopolitical risks (e.g., Caldara and Iacoviello, 2022), economic state evaluations (e.g., Aruoba et al., 2009, and Shapiro et al., 2022), investor sentiment analysis (e.g., Baker and Wurgler, 2007), corporate credit market scrutiny (e.g., Gilchrist and Zakrajšek, 2012), shadow rate investigations (e.g., Wu and Xia, 2016), and considerations of measures related to the COVID-19 pandemic as presented by Arias et al. (2023), along with disruptions in the supply chain discussed by Bai et al. (2024).

The rest of the paper is organized as follows. In Section 2, we examine common empirical indicators of geopolitical fragmentation in the literature. Section 3 introduces a DFM, delving into its specification and estimation intricacies, and produces the geopolitical fragmentation index. Section 4 comprehensively assesses the causal impact of geopolitical fragmentation on economic consequences. Section 5 measures fragmentation in geopolitical blocs by extending the baseline analyses and examines the potentially heterogeneous effects of each bloc's fragmentation. Section 6 concludes. A detailed Appendix provides additional information and robustness exercises.

2 Empirical Indicators of Geopolitical Fragmentation

We compile 14 widely used indicators of geopolitical fragmentation from the literature, each capturing an aspect of the emerging trends. However, no single indicator synthesizes all the relevant information. By combining these indicators using a likelihood-based approach, we aim to extract a more accurate measure of geopolitical fragmentation.

The methodology we present in Section 3 is not dependent on the specific choice of these 14 indicators. Our econometric approach can accommodate more or fewer indicators, and as new indicators become available, we can incorporate them into our index or use them to replace existing ones. Nonetheless, we argue that the 14 indicators we have selected provide a comprehensive survey of existing measures, and our estimates will be robust even if different subsets of these indicators are excluded.

2.1 Data sources for geopolitical fragmentation indicators

We begin by listing each indicator and its sources:

1. The trade openness ratio, (export+import)/GDP, from the International Financial Statistics (IFS).

2. The FDI ratio, calculated as FDI/GDP, from the IFS.
3. The financial flow ratio, (portfolio investment+other investment)/GDP, from the IFS.
4. The migration flow ratio, net migration flows as a percentage of the population, from UN World Population Prospects.
5. The patent flows, from International Patent and Citations across Sectors (INPACT-S) compiled by LaBelle et al. (2023).
6. The number of trade restrictions, from the Global Trade Alert.
7. The capital control measure, from Fernández et al. (2016).
8. The number of sanctions, from Felbermayr et al. (2020).
9. The geopolitical risk index, from Caldara and Iacoviello (2022).
10. The trade policy uncertainty, from Caldara et al. (2020).
11. The energy uncertainty, from Dang et al. (2023).
12. The migration fear index, from Bloom et al. (2015).
13. The number of international conflicts, based on the Uppsala Conflict Data Program.
14. The UN General Assembly Kappa Score: the average of each country-pair, accessible through the datable built by Häge (2017).

The detailed descriptions of the indicators are provided in Appendix C.1. Panel (A) of Figure 1 presents the time series plot for each indicator. Most of the indicators that signal fragmentation (e.g., the capital control measure or the number of sanctions) move upward at the end of the sample, while many of the indicators that measure integration (e.g., trade openness or the financial flow ratio) stagnate. Panel (B) includes informative summary statistics, including the non-stationarity test and pairwise correlations between each indicator and trade openness (calculated using annual aggregated data for the available sample). The main pattern from these correlations is that, although we observe evidence of comovement among indicators, there is also substantial evidence of idiosyncratic behavior. This observation reinforces our motivation of aggregating all indicators into a synthetic one.

Figure 1: Indicators for fragmentation

(A) Time series

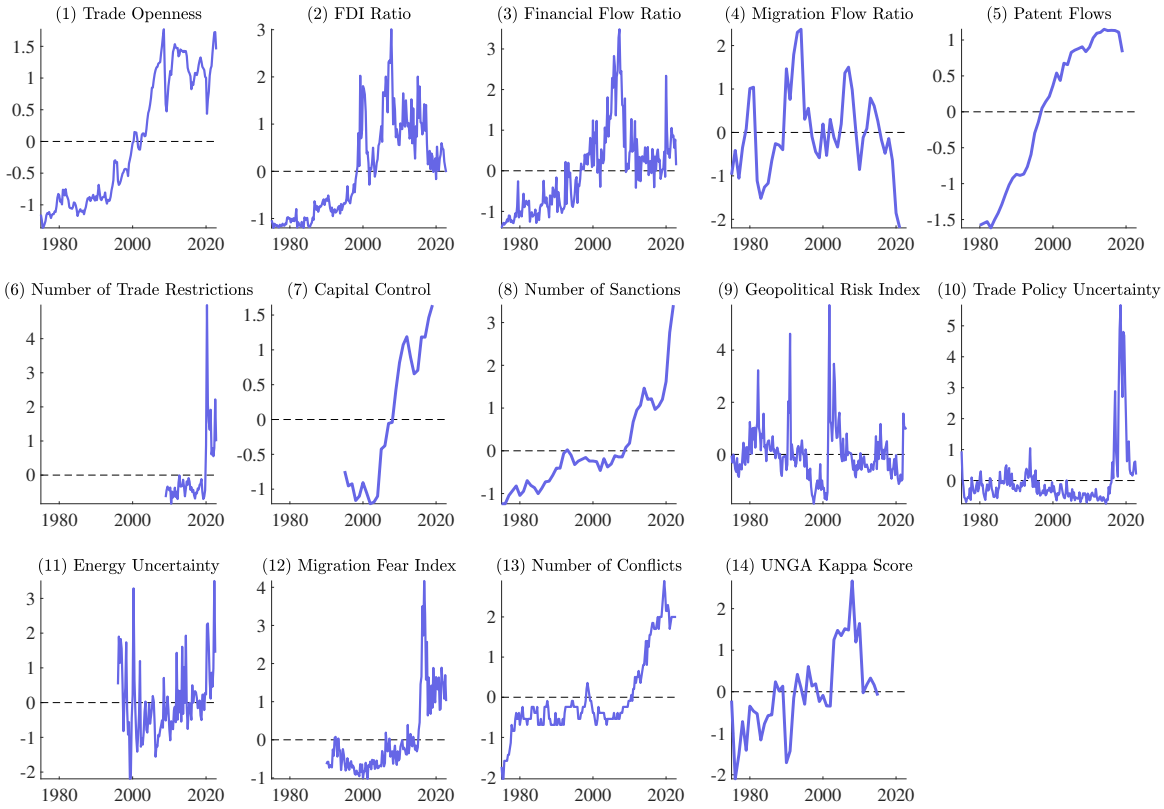

(B) Summary statistics

Category	Individual Indicators	Sample	Freq.	ADF test (p-value)	Correlation w/ Trade Openness
Metrics of economic integration	Trade Openness	1975-2022	Q	0.43	1.00
	FDI Ratio	1975-2022	Q	0.07	0.21
	Financial Flow Ratio	1975-2022	Q	0.05	0.30
	Migration Flow Ratio	1975-2021	A	0.01	0.34
	Patent Flows	1980-2019	A	0.10	0.75
Policy implementation gauges	Number of Trade Restrictions	2009-2022	Q	0.06	0.11
	Capital Control	1980-2019	A	0.71	0.78
	Number of Sanctions	1975-2022	A	1.00	0.66
Text mining-derived indicators	Geopolitical Risk Index	1975-2022	Q	0.00	-0.02
	Trade Policy Uncertainty	1975-2022	Q	0.01	-0.29
	Energy Uncertainty	1996-2022	Q	0.00	0.42
	Migration Fear Index	1990-2022	Q	0.13	0.21
Political reflections	Number of Conflicts	1975-2022	Q	0.37	0.41
	UNGA Kappa Score	1975-2015	A	0.01	-0.63

Notes: See the main text for the sources of each indicator. For comparison purposes, all indicators are standardized to have zero mean and unit standard deviation. Indicators, except those derived from text mining, are the average of all countries with available data. We report the p-value derived from the augmented Dickey-Fuller test, where the null hypothesis assumes non-stationarity.

2.2 Discussion

Next, we offer a literature review summarizing the appeal of our 14 indicators of geopolitical fragmentation and addressing associated caveats. To organize our discussion, we categorize these indicators into four areas: (i) those measuring economic integration, (ii) those gauging policy implementation, (iii) those derived from text mining, and (iv) those offering insights into political dynamics.

2.2.1 Metrics of economic integration

Globalization encompasses the interconnectedness and interdependence of economic and political systems worldwide. Driven by advancements enabling the free flow of goods, services, capital, ideas, and people across borders, its progress is gauged by indicators such as trade openness, FDI, financial flows as a proportion of GDP, migration flow relative to population, and cross-border patent flows (*indicators 1, 2, 3, 4, and 5*). For instance, Aiyar et al. (2023b) and Gopinath (2023) described different phases of globalization using the trade openness metric and pointed out that the remarkable increases in trade since the 1980s have stagnated since 2008. This phenomenon is often referred to as "slowbalization." A similar deceleration is observed in FDI and financial flows. As Gopinath (2023) puts it:

> "Since 2008, however, the pace of globalization has stagnated—the so-called slowbalization—with trade to GDP stabilizing as the forces that helped spur hyperglobalization naturally waned."
>
> (IMF First Managing Deputy Director Gita Gopinath — the 20th World Congress of the International Economic Association, December 2023)

However, interpreting these dynamics requires careful consideration, as several factors, not exclusively tied to globalization or fragmentation, might influence the indicators. For instance, developing countries may witness a decline in trade share due to weak domestic aggregate demand and shifts in economic structures (e.g., the expansion of non-tradable service sectors in developed countries). Moreover, economic and financial cycles play a crucial role in trade, financial, and migration flows.

2.2.2 Policy implementation gauges

The dynamics of macro aggregates partly mirror underlying policy actions aimed at facilitating or impeding international flows, including the imposition or removal of trade restrictions (*indicator 6*) and capital control measures (*indicator 7*). While these policy measures directly impact fragmentation, quantifying them is challenging. Policy measures are often specific to individual countries, and their significance varies based on particular contexts. The literature has devoted much effort to converting qualitative information into quantitative measures.

For instance, Fernández et al. (2016) developed a quantitative measure of a country's capital control strength using diverse information, including qualitative descriptions from the IMF's Annual Report on Exchange Arrangements and Exchange Restrictions (*indicator 7*). Since international flow restrictions may manifest as economic sanctions, Felbermayr et al. (2020) compiled various sanction types, ranging from trade and financial sanctions to military assistance (*indicator 8*).

However, uncertainties persist regarding the scope of policy actions to be considered and the relevance of each measure. Additionally, comprehensive databases may have limited time periods, constrained by the availability of consistently high-quality information over time.

2.2.3 Text mining-derived indicators

Recent advancements in text mining techniques have enabled the extraction of quantitative information from extensive text data. In the realm of geopolitical fragmentation, numerous studies in the literature have crafted indices relevant to fragmentation. These encompass geopolitical events (e.g., war, terrorism, and tensions among countries and political actors) and their associated risks (Caldara and Iacoviello, 2022, *indicator 9*); uncertainty regarding trade policies (Caldara et al., 2020, *indicator 10*); energy uncertainty, often linked to geopolitical tensions (Dang et al., 2023, *indicator 11*); and concerns related to migration flows (Bloom et al., 2015, *indicator 12*). Such indices may capture the latest developments in geopolitical situations or individuals' sentiments about them, which might not be reflected in "hard" data on macroeconomic and financial activities.

2.2.4 Political reflections

Another crucial aspect of fragmentation involves political alignment, where tensions between countries can potentially escalate into violent conflicts. The Uppsala Conflict Data Program provides a comprehensive set of conflict information based on global and local news articles (*indicator 13*). However, political misalignments often do not translate into direct actions against a country. In such instances, previous studies frequently turn to the voting behavior in the United Nations General Assembly (UNGA). These studies gauge the degree of political alignment by assessing the similarity in UNGA voting patterns between countries. Häge (2017) builds on such measures and constructs the "kappa score," which adjusts the observed variability of countries' bilateral voting outcomes based on each country's votes around its average vote (*indicator 14*).

2.3 Taking stock

Our previous discussion highlighted the discernible trends in geopolitical fragmentation apparent across various indicators categorized into four areas. These trends include a global

deceleration in the flows of goods and capital, heightened restrictions on trade and foreign direct investment, increased political risks, sanctions, and conflicts, as well as capital controls and concerns related to migration.

The natural question arises: How can we quantify the dynamics of comovements within this set of empirical indicators and extract the common information present in all of them? A simple average seems unsatisfactory: there is no a priori reason why one indicator should weigh as much as another, and arbitrary weight seems even less appropriate. Can we let the data decide how to weigh each indicator? In the next section, we propose a methodology to address this task.

3 Measuring Geopolitical Fragmentation

In this section, we argue that we can consider the level of geopolitical fragmentation to be an unobservable variable and that each indicator is a noise measure of it. If we take this perspective, we can adopt a likelihood-based approach and let the indicators' dynamics select the optimal weights that will yield an estimate of this unobservable variable.

In particular, we can postulate a flexible DFM with time-varying coefficients and stochastic volatility to account for potential parameter instability and changing uncertainty. Our approach is designed to capture the evolving comovement among time series by allowing their dependence on a common factor to change over time in flexible ways.

Factor models have been integral to the economist's toolkit over an extensive period, notably the unobservable index models proposed by Sargent and Sims (1977) and Geweke (1977). The pioneering work of Stock and Watson (1989) further solidified their significance, aiming to extract valuable information from a broad cross-section of macroeconomic time series for forecasting purposes. Our DFM description builds on the foundations of Del Negro and Otrok (2008) and Del Negro and Schorfheide (2011), utilizing Bayesian techniques for estimation, with particular emphasis on the former addressing potential parameter instability. This Bayesian methodology can be traced back to the influential works of Geweke and Zhou (1996) and Otrok and Whiteman (1998).

3.1 Specification

Let $i \in \{1, ..., N\}$ be the set of indices for the different empirical indicators of geopolitical fragmentation. In our concrete case, $N = 14$, but it could be any other finite natural number, with only the limitation of computational capabilities. The value that each indicator takes at time t is then $y_{i,t}$.

We assume that the dynamics of the $y_{i,t}$ is driven by a common factor f_t:

$$y_{i,t} = a_{i,t} + b_{i,t} f_t + u_{i,t}, \tag{1}$$

which we interpret as the true state of geopolitical fragmentation. In equation (1), the mean $a_{i,t}$, slope $b_{i,t}$, and error $u_{i,t}$ depend both on the empirical indicator and time. In that way, we incorporate much flexibility in how the factor is linked with the empirical indicators.

We assume that $a_{i,t}$ and $b_{i,t}$ evolve as:

$$\begin{aligned} a_{i,t} &= a_{i,0} + a_{i,1} t, \\ b_{i,t} &= b_{i,t-1} + \sigma_{b_i} \epsilon_{b_i,t}, \quad \epsilon_{b_i,t} \sim \mathcal{N}(0,1). \end{aligned}$$

First, we address non-stationarity in the proxies $y_{i,t}$ by incorporating a deterministic time trend $a_{i,t}$ orthogonal to the common factor f_t. This is crucial, as demonstrated in Panel (B) of Figure 1, where some indicators exhibit non-stationarity while others do not. The assumption underlying our approach is that the common dynamics across empirical indicators are captured by their stationary or cyclical components. Second, we accommodate time-varying sensitivities $b_{i,t}$ of individual proxies with respect to the common factor f_t through a random-walk process, capturing potential slow-moving variations. Our goal is to allow their dependence on the factor to evolve. This flexibility is crucial, as certain indicators may reveal more about geopolitical fragmentation than others, and their importance can change dynamically over time.

In comparison, we model the evolution of the factor and the error as autoregressive processes:

$$\begin{aligned} f_t &= \phi_{f,1} f_{t-1} + ... + \phi_{f,p} f_{t-p} + \sigma_{f,t} \epsilon_{f,t}, \quad \epsilon_{f,t} \sim \mathcal{N}(0,1), \\ u_{i,t} &= \phi_{u_i,1} u_{i,t-1} + ... + \phi_{u_i,q} u_{i,t-q} + \sigma_{u_i,t} \epsilon_{u_i,t}, \quad \epsilon_{u_i,t} \sim \mathcal{N}(0,1). \end{aligned}$$

We allow the individual error terms $u_{i,t}$ to exhibit serial correlation, capturing dynamics that do not comove and are idiosyncratic to each series. This approach involves relaxing the assumption that all dynamics arise solely from the factor. The rationale behind this adjustment is to prevent the factor estimates from becoming overly dependent on a subset of empirical indicators that exhibit high persistence.

Finally, all the innovation variances, denoted by $\sigma_{k,t}$, are stochastic and display time-varying characteristics:

$$\begin{aligned} \sigma_{k,t} &= \sigma_k \exp(h_{k,t}), \\ h_{k,t} &= h_{k,t-1} + \sigma_{h_k} \epsilon_{h_k,t}, \quad \epsilon_{h_k,t} \sim \mathcal{N}(0,1), \quad k \in \{f, u_1, ..., u_N\}. \end{aligned}$$

This attribute holds for both the innovations to the common factor and those associated with the idiosyncratic error terms. The incorporation of stochastic volatility is crucial not only for modeling the non-Gaussian features inherent in the data, but also for effectively capturing potential outlier events that may occur in certain years, both for the factor and the idiosyncratic terms. This dynamic approach allows the model to adapt to changing volatility patterns, offering a more robust representation of the underlying dynamics in the empirical indicators.

Compiling all the previous equations for easy reference, we get the complete specification of our DFM:

$$
\begin{aligned}
y_{i,t} &= a_{i,t} + b_{i,t} f_t + u_{i,t}, \\
a_{i,t} &= a_{i,0} + a_{i,1} t, \\
b_{i,t} &= b_{i,t-1} + \sigma_{b_i} \epsilon_{b_i,t}, \quad \epsilon_{b_i,t} \sim \mathcal{N}(0,1), \\
f_t &= \phi_{f,1} f_{t-1} + ... + \phi_{f,p} f_{t-p} + \sigma_{f,t} \epsilon_{f,t}, \quad \epsilon_{f,t} \sim \mathcal{N}(0,1), \\
u_{i,t} &= \phi_{u_i,1} u_{i,t-1} + ... + \phi_{u_i,q} u_{i,t-q} + \sigma_{u_i,t} \epsilon_{u_i,t}, \quad \epsilon_{u_i,t} \sim \mathcal{N}(0,1), \\
\sigma_{k,t} &= \sigma_k \exp(h_{k,t}), \\
h_{k,t} &= h_{k,t-1} + \sigma_{h_k} \epsilon_{h_k,t}, \quad \epsilon_{h_k,t} \sim \mathcal{N}(0,1), \quad k \in \{f, u_1, ..., u_N\}.
\end{aligned} \tag{2}
$$

3.2 Priors

Our priors for the model parameters in (2) exhibit symmetry across a range of empirical indicators related to geopolitical fragmentation $i \in \{1, ..., N\}$:

$$
\begin{aligned}
a_i = \begin{bmatrix} a_{i,0} \\ a_{i,1} \end{bmatrix} &\sim \mathcal{N}\left(\begin{bmatrix} 0 \\ 0 \end{bmatrix}, \begin{bmatrix} 1 & 0 \\ 0 & \frac{1}{2} \end{bmatrix} \right), \\
\phi_k &\sim \mathcal{N}\left(\frac{1}{2}, \frac{1}{2} \right), \\
\sigma_{b_i}^2 &\sim \mathcal{IG}\left(10, \frac{1}{10} \right), \\
\sigma_g^2 &\sim \mathcal{IG}\left(1, 1 \right),
\end{aligned} \tag{3}
$$

where $k \in \{f, u_i\}$ and $g \in \{u_i, h_f, h_{u_i}\}$.

We intentionally pick loose priors to introduce greater flexibility and reduce the sensitivity of estimation results to the choice of prior distributions. Our priors embody the belief that the degree of time variation in the factor loading $\sigma_{b_i}^2$ is relatively smaller in comparison to the variations in the idiosyncratic error terms or the stochastic volatilities. However, for both cases, the weight of the prior relative to the sample for variances is not adjusted, leading to a substantial reduction in the impact of the prior as the sample length increases. We

additionally explore a scenario wherein the factor loading b_i remains constant over time, and we adopt a loose prior, which is centered around one with a substantial variance of $\mathcal{N}\left(1, \frac{1}{2}\right)$. Below, we will discuss the robustness of our results to different priors.

3.3 Estimation

The estimation procedure for our DFM utilizes a Gibbs sampler to draw samples from the exact finite sample joint posterior distribution of both the parameters and the latent state variables, including the common factor. We extend the Gibbs sampler initially proposed by Del Negro and Otrok (2008), focusing on addressing the challenges associated with handling missing data and discrepancies in data frequencies, specifically pertaining to stock variables rather than flow variables. Appendix A presents a comprehensive description of the modifications we introduce.

In terms of concrete specification, we set the lag order for f_t and $u_{i,t}$ to be one, and we pick the time frame for our 14 indicators to be from 1975:Q1 to 2022:Q4. We also standardized them to have zero sample mean and unit standard deviation. The purpose of this standardization is to ensure that all the indicators contribute to the measurement of geopolitical fragmentation comparably. The trade openness ratio, the FDI ratio, the financial flow ratio, the migration flow ratio, and the patent flows undergo an adjustment by multiplication with -1 to account for their inverse correlation with the underlying object of interest. This adjustment facilitates the imposition of symmetric priors for factor loading across the various empirical indicators.

In instances where data are only accessible on an annual basis, the variables are characterized as stock rather than flow variables. These variables capture values at specific points in time, much like snapshots of the economy. Handling missing observations in this context is straightforward as discussed in Aruoba et al. (2009). For the annual series, we assume that the individual error terms associated with them are not serially correlated.

In equation (1), there exist three sets of latent states: f_t, $b_{i,t}$, and $h_{k,t}$. All of these necessitate initialization or normalization. To mitigate the indeterminacy concerning sign and magnitude for factor loadings $b_{i,t}$ and factor levels f_t, we initialize the values for $b_{i,0}$ to one. The initialization values for f_0 and $h_{k,0}$ are set to zero, with the specific value for f_0 being non-crucial. In addition, we set the variance of innovation to the common factor to one, denoted as $\sigma_f = 1$. Del Negro and Otrok (2008) present a more comprehensive discussion on the identification of a DFM with time-varying loadings and stochastic volatilities.

3.4 Results

In Figure 2, we display the posterior median (smoothed) estimates of f_t, our geopolitical fragmentation index, alongside 90% credible intervals. To aid interpretation, we overlay

major historical events influencing globalization. For space efficiency, the posterior estimates for the remaining unknowns in the model can be found in Appendix D.1. As shown in Figure 1, certain indicators were unavailable until the mid-1990s, leading to wider credible intervals up to that period. Thus, our estimate is more sensitive to individual indicators during the initial periods from 1975 to 1995 but becomes more robust post-1995.

Figure 2: Estimated fragmentation index

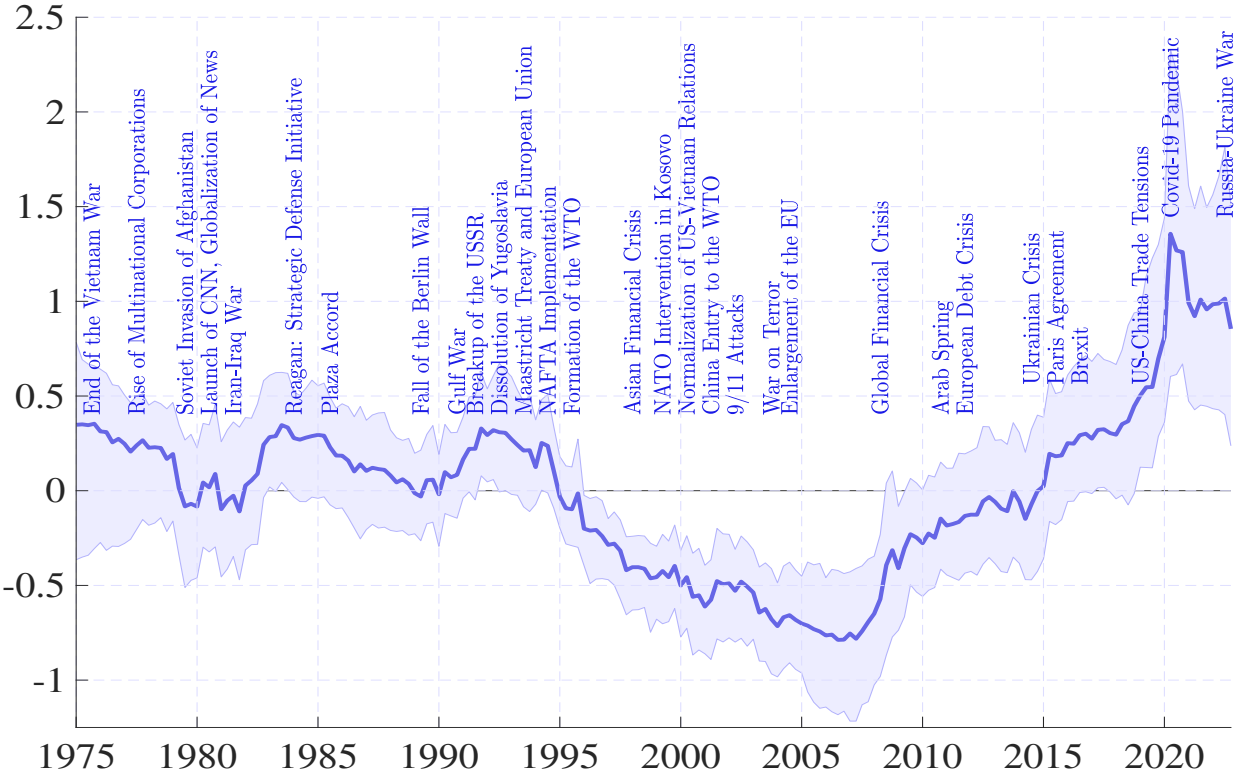

Notes: Posterior median-smoothed estimates of f_t accompanied by 90% credible intervals. We overlay with major historical events.

Our estimated fragmentation index aligns well with the narrative understanding of geopolitical fragmentation, as noted in Gopinath (2023). Our median estimate of fragmentation was stable between 1975 and the early 1990s. While trade openness was increasing, the world economy was still divided between the market economies and socialist economies blocs. Other indicators, like the FDI ratio or the financial flow rate, did not show much of an upward trend.

Starting from the mid-1990s, our index reports an upward trajectory in globalization. Key events contributing to this trend include the breakup of the Soviet Union, the Maastricht Treaty and the formation of the European Union, the establishment of the World Trade Organization (WTO), and China's entry into the WTO. In fact, these were the years when the term "globalization" became popular outside of economics.

This trend shifted post-2008, experiencing a notable upswing coinciding with the 2007-2008 financial crisis. The subsequent decade witnessed a significant surge, reflecting heightened challenges in global trade and capital flows driven by geopolitical events (e.g., conflicts, trade tensions) and the global pandemic. The process of geopolitical fragmentation has not reverted by the end of the sample, although there are some weak indications of a slowdown in fragmentation after the end of the worst phase of the COVID-19 pandemic.

3.5 Robustness checks

Next, we demonstrate the robustness of our DFM estimation results by showcasing their consistency across alternative selections of indicators and prior choices.

Figure 3: Estimated fragmentation index: Alternative selection of indicators and prior choices

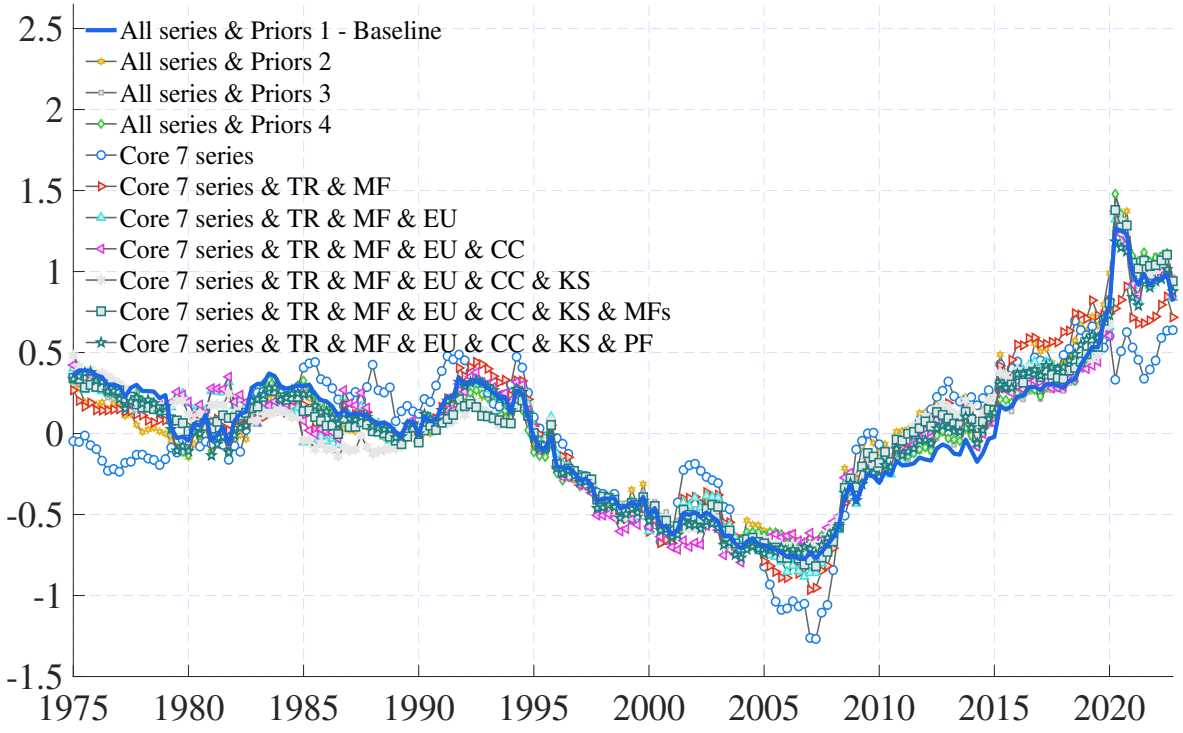

Notes: Median-smoothed estimates of the fragmentation index under our baseline specification and ten variations.

Figure 3 plots the median estimate of our baseline specification plus a set of ten variations. We ensure consistency by scaling all lines to match the standard deviation of the baseline case. This allows for straightforward comparison across all lines. For clarity, we designate the baseline scenario as "All series & Priors 1," indicating our utilization of all 14 series of indicators in Figure 1 and adherence to the prior choices outlined in (3).

Now, we explain the different lines. First, we examine three distinct sets of prior selections for the variance parameters listed below while preserving all 14 series. We focus exclusively

on adjusting priors for the variance parameters, as the priors for the remaining parameters have already been set to sufficiently broad values.

The rationale for organizing these choices according to their importance level is as follows. First, varying options for $\sigma^2_{b_i}$ are critical as they dictate the degree of time variations in the factor loading, thereby influencing our estimation outcomes. Second, the priors for $\sigma^2_{u_i}$ directly impact the signal-to-noise ratio by determining the variance magnitude of the unexplained idiosyncratic component, rendering them potentially significant for estimation. Last, the priors for $\sigma^2_{h_f}$ and $\sigma^2_{h_i}$ regulate the extent of time variations in stochastic volatility, consequently affecting the signal-to-noise ratio. Specifically, we consider:

$$
\begin{aligned}
&\text{Priors 2:} && \sigma^2_{b_i} \sim \mathcal{IG}(10,1), && \sigma^2_{u_i} \sim \mathcal{IG}(10,10), && \sigma^2_{h_f}, \sigma^2_{h_i} \sim \mathcal{IG}(10,10),\\
&\text{Priors 3:} && \sigma^2_{b_i} \sim \mathcal{IG}(10,0.1), && \sigma^2_{u_i} \sim \mathcal{IG}(1,2), && \sigma^2_{h_f}, \sigma^2_{h_i} \sim \mathcal{IG}(10,1),\\
&\text{Priors 4:} && \sigma^2_{b_i} \sim \mathcal{IG}(10,0.1), && \sigma^2_{u_i} \sim \mathcal{IG}(1,0.5), && \sigma^2_{h_f}, \sigma^2_{h_i} \sim \mathcal{IG}(10,1).
\end{aligned}
$$

Subsequently, having gauged the implications of alternative prior choices for estimation outcomes, we revert to the prior choices for the baseline scenario as delineated in equation (3), and examine variations in the set of indicators. The "Core 7" denotes the scenario wherein we exclusively utilize trade openness, the FDI ratio, the financial flow ratio, the number of sanctions, the geopolitical risk index, the trade policy uncertainty, and the number of conflicts.[1] Next, we incrementally incorporate (in different combinations) the number of trade restrictions (TR), the migration fear index (MF), the energy uncertainty (EU), the capital control (CC), the UNGA kappa score (KS), the migration flow ratio (MFs), and the patent flows (PF).

Figure 3 juxtaposes the median-smoothed estimates of the fragmentation index across these adjustments. Remarkably, the time-series plots of our estimated fragmentation index remain highly similar throughout these modifications. They consistently depict a robust correlation, averaging approximately 0.95, with the lowest observed correlation hovering around 0.85. This compelling evidence strongly reinforces our assertion that a specific set of empirical indicators does not influence the estimation but rather that it captures the underlying dynamics of fragmentation.

4 The Causal Effects of Geopolitical Fragmentation

Having estimated an index summarizing the extent of geopolitical fragmentation, we can now delve into exploring the causal link between geopolitical fragmentation and global economic activity.

[1] We call these indicators the "Core 7" owing to their quarterly frequency availability throughout the entire estimation period from 1975 to 2022.

Our investigation employs two widely accepted empirical techniques for causality assessment in time series: structural vector autoregressions (SVARs) and local projection (LPs). SVARs and LPs are alike in their fundamental nature, estimating dynamic relationships among observed variables within a linear projection model class; see Plagborg-Møller and Wolf (2021). In a finite sample and under model specification uncertainty, SVARs efficiently regulate the structure of relationships among variables. Conversely, LPs offer a more flexible model specification framework, exhibiting resilience against the curse of dimensionality. Their complementarities justify the use of both approaches to have a more complete assessment of the causal effects of geopolitical fragmentation.

We apply SVARs and LPs to quarterly panel data, covering a comprehensive set of macro and financial variables across a total of 61 economics: 34 advanced economies (AEs) and 27 emerging markets (EMs) with available data. Appendix D.2 provides descriptive statistics for these variables.

We begin with a panel SVAR to scrutinize the impact of fragmentation on a country's macro and financial variables. Afterward, we transition to a panel LP analysis to explore potential heterogeneity across the sample. We complete our empirical investigation with a sectoral impact employing LPs.

4.1 Aggregate impact: A panel SVAR approach

The panel SVAR comprises 11 variables categorized into global and country components. The global block encompasses (i) our geopolitical fragmentation index, (ii) the VIX, (iii) the log of the S&P 500 index, (iv) the log of the WTI price of oil, (v) the yield on two-year U.S. Treasuries, (vi) the Chicago Federal Reserve National Financial Conditions Index (NFCI), and (vii) the log of world real GDP, aligning with the variable selection methodology of Caldara and Iacoviello (2022). The global variables control for the interactions between the fragmentation index and the aggregate variables of a country, aiding in the identification of causal effects of shocks to the fragmentation index. Notably, U.S. financial market indicators are treated as "global" variables due to their influential role in the global market. The country block consists of (viii) the log of a country's stock price index (SP_{it}), (ix) the industrial production index (IP_{it}), (x) the log of fixed investment (I_{it}), and (xi) the log of per capita GDP (GDP_{it}).[2]

The SVAR incorporates two lags and utilizes quarterly data spanning from 1986:Q1 to 2022:Q4, with the starting point of the sample determined by the availability of the VIX. To

[2]For each country, we construct

$$Y'_{it} = \begin{bmatrix} \text{Fragmentation Index}_t, & \text{VIX}_t, & \ln(\text{S\&P}_t), & \ln(\text{WTI}_t), & \text{U.S. Treasury}_t, & \text{NFCI}_t, \\ \ln(\text{World GDP}_t), & \ln(\text{SP}_{it}), & \text{IP}_{it}, & \ln(\text{I}_{it}), & \ln(\text{GDP}_{it}) & \end{bmatrix} \quad (4)$$

for the panel VAR estimation.

capture country-specific factors, the panel SVAR is estimated with country fixed effects (FEs). Data are sourced from the IMF International Financial Statistics (IFS), and observations with changes from the previous period in the top or bottom 1.25th percentile are excluded as outliers. The sample, constituting an unbalanced panel, consists of 2,359 observations from 26 countries (17 AEs and 9 EMs). The sample size is smaller than in the subsequent LP analysis, since VARs necessitate the availability of all variables simultaneously. At the same time, LPs can be executed for each variable independently, resulting in more observations for regressions.

Standard errors are clustered by time due to the absence of cross-sectional variations in global variables. A fragmentation shock is identified through Cholesky decomposition, with the fragmentation index ordered first. This identification assumption relies on the hypothesis that geopolitical fragmentation is driven more by low-frequency forces (e.g., changes in international relations driven by demographics or ideological shifts) than by contemporary quarterly shocks to aggregate economic variables.

Figure 4: Economic impact of fragmentation: SVAR

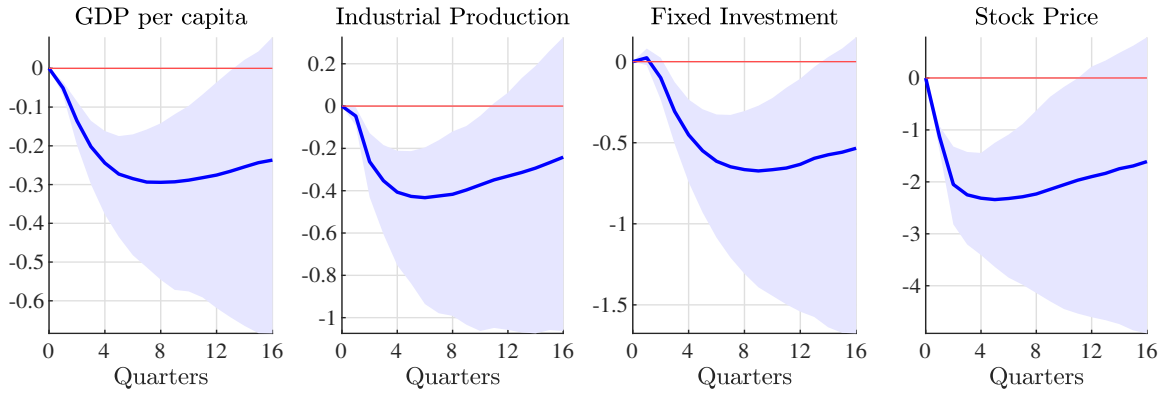

Notes: Derived from a combined sample of AEs and EMs. Percent responses to a one-standard-deviation fragmentation shock. Shaded areas indicate the 90th percentiles where standard errors are clustered by time.

Figure 4 presents the impulse response functions (IRFs) of country variables to a one-standard-deviation fragmentation shock. Given the assumption of identical coefficients in the VAR system across countries, these IRFs can be interpreted as the average effects of a fragmentation shock within the sample. Following a positive innovation to the fragmentation index (deemed adverse), all four country variables—GDP per capita, industrial production, fixed investment, and stock prices—experience declines. The negative effects become most pronounced approximately one to two years after the initial shock. The impact is substantial and persistent, with the peak effect of a one-standard-deviation fragmentation shock resulting in approximately a 0.3% decline in GDP.

4.2 Assessing the robustness of SVAR results

Next, we report the key findings of our robustness checks. Appendix D.3 provides many more details. Despite different prior choices or reliance on different sets of empirical indicators, the consistency in SVAR outcomes across these variations strengthens the credibility of our findings.

4.2.1 Examination of estimation modifications

We assess the robustness of our results by systematically examining various estimation modifications. In addition, we investigate a scenario where trade openness serves as the sole indicator for geopolitical fragmentation, a common practice in the literature. Our findings reveal that adverse shocks to trade openness, indicative of increased fragmentation, indeed exert a negative impact on economic activity. Yet, this impact is markedly transitory, enduring only up to one year and displaying subsequent mean reversion (Appendix Figure A-6). In contrast, our baseline results unveil a divergent narrative, highlighting the prolonged persistence of observed effects for an extended duration, exceeding three to four years. This suggests that our fragmentation measure presents a materially different picture, which holds greater significance for the global economy.

4.2.2 Imposing alternative identification strategies

We assess the robustness of our SVAR results by employing two alternative identification strategies: switching the Cholesky ordering and a narrative approach.

First, we change the ordering of variables in the Cholesky decomposition. This approach gauges the importance of our identification assumption. Panel (A) of Figure 5 presents the IRFs in which the fragmentation index is ordered last in the Cholesky ordering. One can think about this ordering as the worst-case scenario for the hypothesis that fragmentation shocks matter. More concretely, this assumption implies that fragmentation shocks do not have any contemporaneous impacts on global or country variables.

Not surprisingly, under this assumption, the magnitude of the IRFs diminishes, as anticipated, compared to the baseline case where the fragmentation index is placed first in the Cholesky ordering. However, most variables still indicate a significant effect of fragmentation shocks and the shape of responses remains qualitatively unchanged. Appendix D.3 presents the results with alternative orderings and confirms that they lie between the two scenarios depicted in Figure 5.

Our second identification strategy employs narrative restrictions in the tradition of Mertens and Ravn (2013). We identify significant fragmentation and globalization episodes and employ them as external instruments for fragmentation shocks. To ensure orthogonality with all other shocks, we select episodes that are unexpected or unrelated to the state of the global

Figure 5: Economic impact of fragmentation: Assessing SVAR results robustness

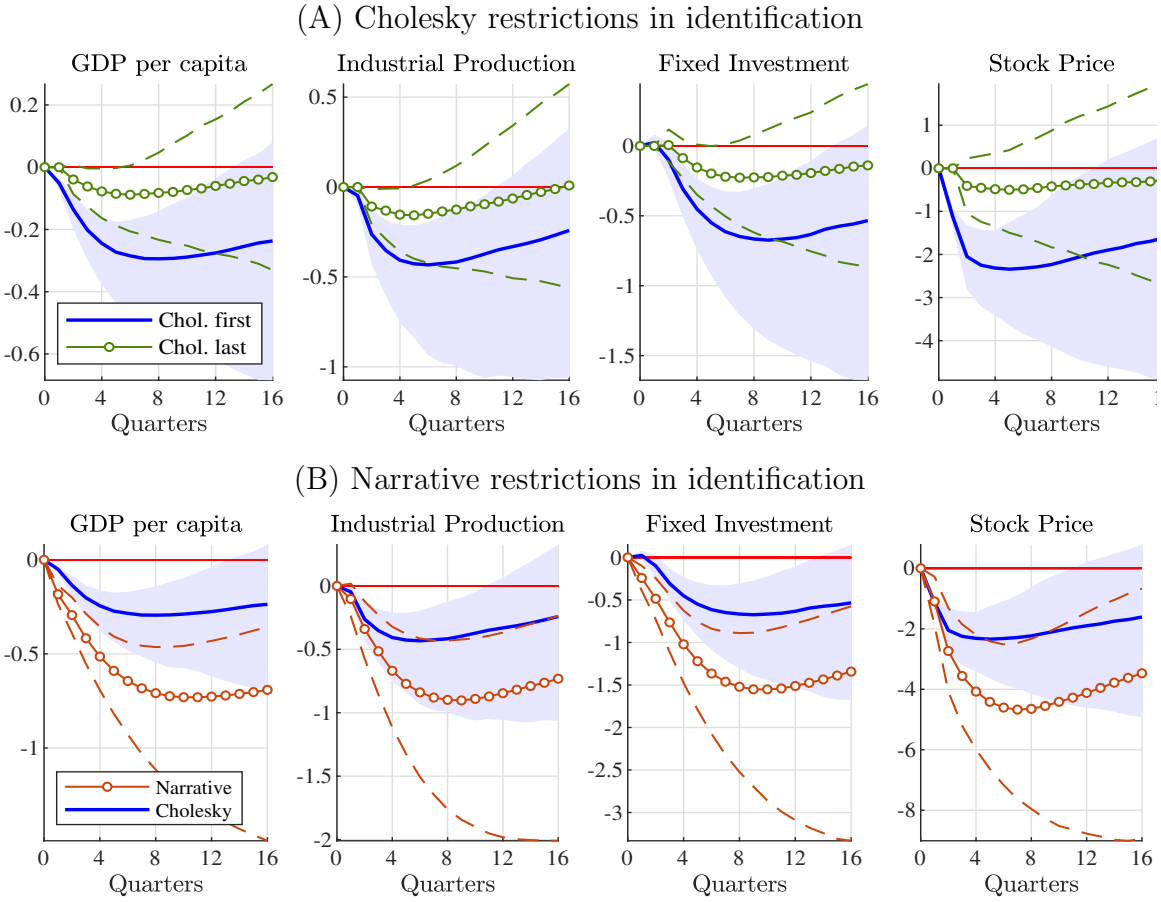

Notes: Derived from a combined sample of AEs and EMs. Percent responses to a one-standard-deviation fragmentation shock. Shaded (dashed) areas indicate the 90th percentiles where standard errors are clustered by time. Panel (A): Blue and green lines display the IRFs in which the fragmentation index is ordered first and last in the Cholesky decomposition, respectively. The ordering of other variables is kept unchanged. Panel (B): The blue line shows the baseline case of the Cholesky decomposition with the fragmentation index ordered first. The red is obtained through the narrative restrictions described above.

economy. Consequently, events that influenced fragmentation but were rooted in global economic conditions or directly impacted them, such as the 2007-2008 financial crisis and the COVID-19 pandemic, are excluded.

Table 1 lists the narrative episodes we select, categorized into three sections. Comprehensive details of these episodes are available in Appendix C.3. Narrative events reflecting on geopolitical fragmentation (globalization) are indicated with an asterisk (dagger). We assign a value of 1 to events reflecting on fragmentation and -1 to those reflecting on globalization. There is a correlation of approximately 0.15 between the reduced-form residuals of the VAR model and the narrative series.

Panel (B) of Figure 5 plots the IRFs of a fragmentation shock instrumented by the nar-

Table 1: Narrative episodes: Reflecting on geopolitical fragmentation

(A) Surprise war outbreaks, international conflicts, terrorism
Iraqi invasion of Kuwait* (1990:Q3), Gulf War* (1991:Q1), NATO intervention in Serbia* (1994:Q2) and Kosovo* (1999:Q1), 9.11* (2001:Q3), Iraq War* (2003:Q1), U.S. strike on ISIL* (2014:Q3) and its breakup†(2017:Q4), Russian invasion of Ukraine* (2022:Q1)
(B) Unforeseen geopolitical shifts
Fall of the Berlin Wall†(1989:Q4), USSR dissolution events†(1988-1991), Arab Spring* (2010:Q4), Brexit vote* (2016:Q2)
(C) Enactment of trade deals, currency unions, or trade restrictions
NAFTA†(1994:Q1), WTO†(1995:Q1), Mercosur†(1995:Q1), Euro†(1999:Q1), U.S.-China trade war* (2018-2019)

Notes: See Table C.3 for more details. We list 18 events, but we further break down historical occurrences, such as the dissolution of the USSR and the U.S.-China trade war, into multiple events. Hence, we present a total of 22 narrative episodes. Narrative episodes reflecting on geopolitical fragmentation (globalization) are marked with an asterisk (dagger). For (C), while these events were typically agreed upon or announced beforehand, their implementation signifies material alterations in measures that impact economic activities. We verified that the exclusion of events under category (C) does not affect our result.

rative series.[3] Notably, the impacts are considerably larger compared to the baseline case, leading to a 0.7% decline in GDP per capita in response to a one-standard-deviation shock. This outcome suggests the presence of measurement errors in the fragmentation index, which are effectively corrected by the instruments.

Taken together, our two alternative identification strategies underscore the robustness of our SVAR results under a reasonable set of identification assumptions.

4.3 Aggregate impact: A panel LP approach

We implement a panel LP by estimating the following equation:

$$y_{i,t+h} - y_{i,t-1} = \beta^h s_t + \sum_{l=1}^{L} \alpha_l^h \Delta y_{i,t-l} + \sum_{l=1}^{L} \gamma_l^h s_{t-l} + \delta^h X_{i,t} + \mu_i^h + \epsilon_{i,t}^h, \tag{5}$$

[3]The first stage regression is conducted by regressing the VAR reduced-form residuals on narrative series. $u_{it}^f = \underset{(0.012)}{-0.004} + \underset{(0.030)}{0.080}\ z_t + e_{it}$, where u_{it}^f is the residuals of the fragmentation index obtained from the panel VAR, and z_t is the narrative series. Standard errors are clustered by time and shown in parentheses. The coefficient of the narrative series is significant at the 1% level. The second stage takes steps described by Mertens and Ravn (2013).

for $h = 0, 1, 2, ...$ where $y_{i,t+h}$ represents the outcome variable in country i at time $t+h$, i.e., $y_{i,t+h} = \{\ln(\text{GDP}_{it+h}), \text{IP}_{it+h}, \ln(\text{I}_{it+h}), \ln(\text{SP}_{it+h})\}$, and s_t is the fragmentation shock obtained in the SVAR. However, it is crucial to highlight the robustness of our results to alternative identification schemes, as illustrated in Appendix D.3.5. Following Montiel Olea and Plagborg-Møller (2021), we include lagged outcome and explanatory variables, $\Delta y_{i,t-l}$ and s_{t-l}, to address serial correlation, choosing a lag length of two.

In terms of regressors, $X_{i,t}$ is a vector of global and country-specific controls, encompassing the first and second lagged terms of a country's per capita GDP growth rate and the global variables used in the VAR analysis, i.e., the VIX, the S&P 500 index, the WTI oil price, the yield on two-year U.S. Treasuries, the NFCI, and world GDP. The WTI oil price and world GDP are taken as log-difference. μ_i^h denotes country FEs and $\epsilon_{i,t}^h$ is an error term. Standard errors are clustered by time, as in the SVAR.

The sequence of estimated coefficients, β^h for $h = 0, 1, 2, ...$, represents the IRFs. The estimation period t extends until 2019:Q4 to ensure a consistent sample across the horizon h. We run the regression for each country variable separately. The number of observations differs across variables depending on data availability: 5,543 for GDP per capita (34 AEs / 27 EMs), 4,153 for industrial production, 5,010 for fixed investment, and 2,430 for stock prices in the longest horizon of the estimation ($h = 16$).

As depicted in Panel (A) of Figure 6, a fragmentation shock exhibits adverse effects on country variables, showing qualitative similarity to the SVAR result. Notably, the estimated magnitude is somewhat larger in the LP analysis. For instance, the peak response of GDP per capita is approximately 0.9%. This variance is partly attributed to the broader inclusion of EMs in the sample.

In Panels (B)-(F) of Figure 6, we investigate state dependence across country and shock characteristics by incorporating distinct coefficients, thus examining variations in the regression outcomes for different countries and shocks categorized as positive versus negative:

$$\begin{aligned} y_{i,t+h} - y_{i,t-1} = & \left[\mathbf{1}_{i,t-1}\beta_1^h + (1 - \mathbf{1}_{i,t-1})\beta_0^h\right] s_t \\ & + \sum_{l=1}^{L} \alpha_l^h \Delta y_{i,t-l} + \sum_{l=1}^{L} \gamma_l^h s_{t-l} + \delta^h X_{i,t} + \mu_i^h + \epsilon_{i,t}^h, \end{aligned} \tag{6}$$

where $\mathbf{1}_{i,t}$ is an indicator variable that takes one for the sample with a specific characteristic of our interest.

In Panel (B), fragmentation negatively impacts both AEs and EMs. Notably, the adverse repercussions are more pronounced for EMs. This suggests that countries with lower income levels experience more severe consequences from fragmentation, indicating greater potential benefits from globalization.

Transitioning to Panel (C), we classify sample countries based on their voting patterns

Figure 6: Economic impact of fragmentation: LP

(A) All countries

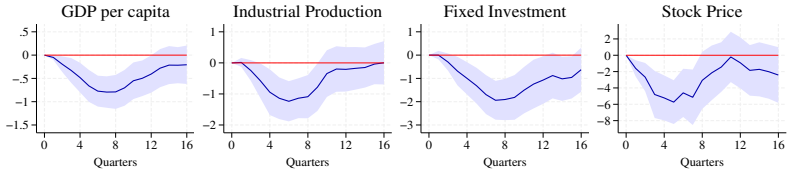

(B) AEs (**red**) versus EMs (**blue**)

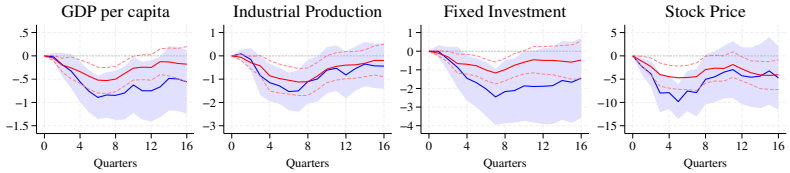

(C) West (**red**) versus East (**blue**)

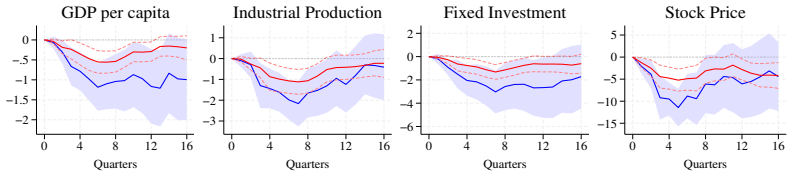

(D) High trade share (**red**) versus other countries (**blue**)

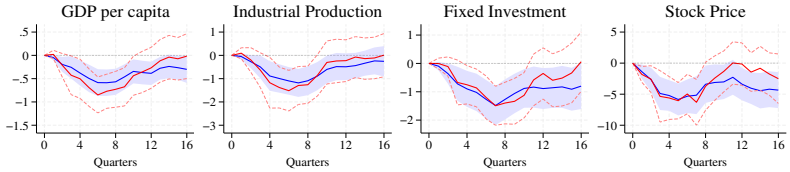

(E) High trade share with U.S. (**red**) versus other countries (**blue**)

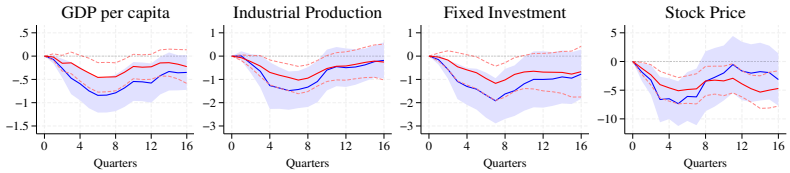

(F) Fragmentation (**red**) versus globalization (**blue**): All countries

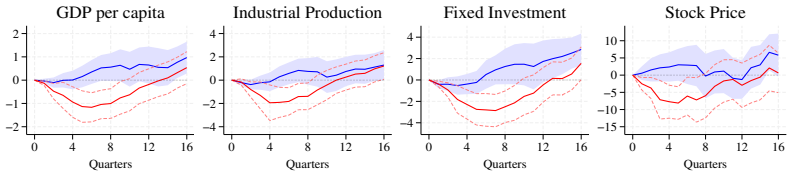

Notes: Percent responses to a one-standard-deviation fragmentation shock. Shaded areas and dashed lines indicate the 90th percentiles. In Panel (A), all countries include AEs and EMs. In Panel (B), AEs and EMs follow the classification of the IMF World Economic Outlook. In Panel (C), the term "West" encompasses countries that supported the United Nations General Assembly Resolution on March 2, 2022 (ES-11/1), while "West" comprises countries that either voted against the resolution or abstained. In Panel (D), countries with trade share are defined as those with (export+import)/GDP above the median of the sample. In Panel (E), the trade share with the U.S. is calculated using country-pair trade flows in the BACI database. In Panel (F), a positive shock to the fragmentation index is denoted as a "fragmentation" shock, while a negative shock is referred to as a "globalization" shock.

in the United Nations General Assembly Resolution on March 2, 2022, condemning Russia's aggression against Ukraine. The "East" group, comprising nations like Russia, China, India, and South Africa, which either opposed or abstained from voting on the resolution, exhibits more substantial declines in the aftermath of a fragmentation shock. This result is interesting as these nations are less supportive of a rules-based international order from which they benefit more.

In Panels (D) and (E), we explore the relationship between the impact of fragmentation shocks and a country's trade openness, measured by the trade share (i.e., the sum of exports and imports relative to GDP). Panel (D) highlights that nations with higher trade shares are more susceptible to the effects of fragmentation shocks. Conversely, a reversal is observed when trade openness is linked to the U.S. Panel (E) shows that countries with higher trade shares with the U.S. exhibit lower vulnerability to the impacts of fragmentation shocks.

Lastly, Panel (F) delves into disparities between positive (fragmentation) and negative (globalization) shocks by estimating these IRFs separately in the state-dependency regression (6). This figure illustrates that fragmentation shocks exert immediate adverse impacts on the global economy, whereas the effects of globalization shocks unfold gradually over 2 to 3 years, demonstrating greater persistence.

4.4 Sectoral impact: A panel LP approach

4.4.1 OECD countries

So far, we have shown that fragmentation has adverse effects on the overall economy. Our focus now shifts to examining how fragmentation influences various sectors within a country, with a particular emphasis on OECD countries.

The OECD conducts an annual breakdown of GDP across ten major sectors, aligning closely with the 2-digit U.S. Standard Industrial Classification (SIC) system used in the subsequent section. This GDP breakdown covers the 38 OECD member countries. Utilizing VAR-identified fragmentation shocks and employing the set of control variables from the preceding section, we perform a panel LP analysis of (5). The dataset, an unbalanced panel, spans from 1986 to 2022, with most countries' data becoming available only in the late 1990s.

Panel (A) of Figure 7 reports the responses at impact to a fragmentation shock to sectoral GDP in OECD countries. Sectors with greater exposure to global economic and financial activities, such as manufacturing, construction (investment activities), wholesale and retail trade, information and communication, and professional services, demonstrate more pronounced responses. In contrast, domestically oriented sectors like agriculture, forestry, and fishing, real estate, and public services exhibit muted reactions. Importantly, this discernible sectoral pattern is also observed in the case of the U.S. economy, a point we delve into in the following section.

Figure 7: Fragmentation impact on sectoral GDP

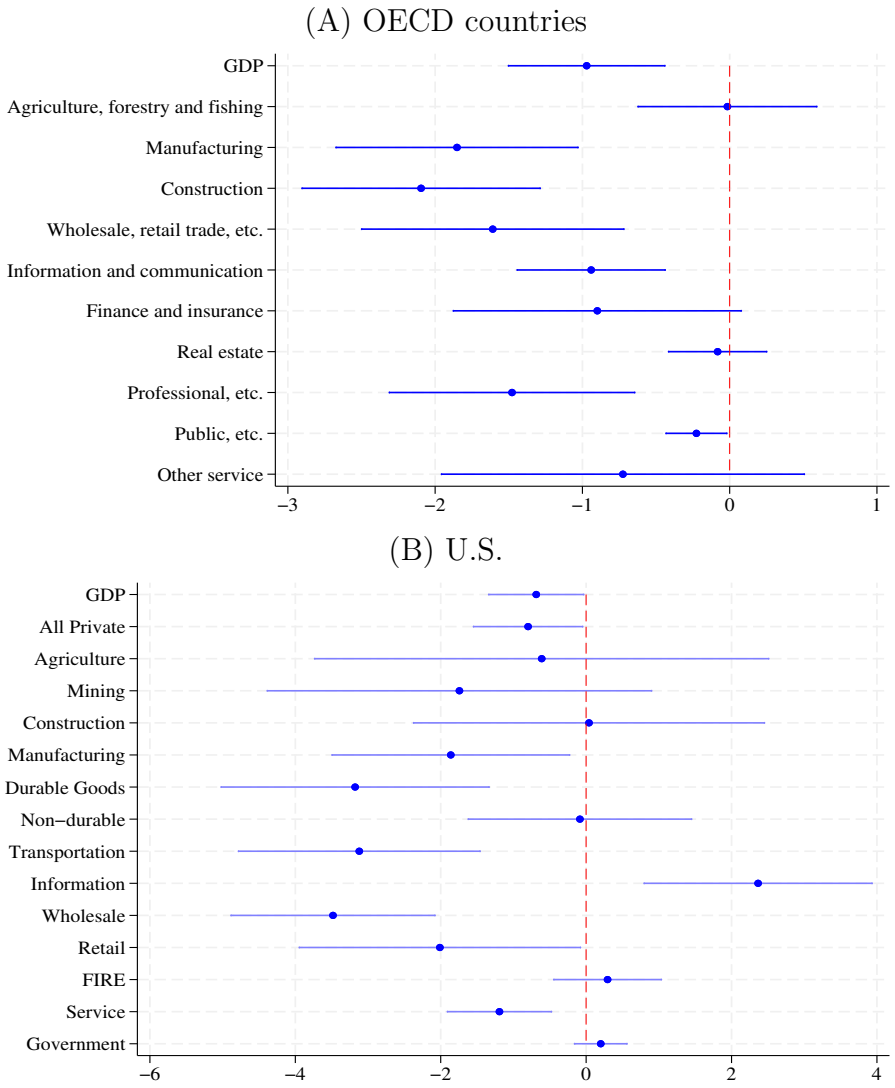

Notes: Panel (A): Sample of 38 OECD countries. Percent responses of 1-year ahead GDP to a one-standard-deviation shock to the factor. Bars indicate the 90th percentiles. "Wholesale, retail trade, etc." includes wholesale, retail trade, repairs, transport, accommodation, and food services. "Professional, etc." represents professional, scientific, and support services. "Public, etc." is the sum of public administration, defense, education, health, and social work. Panel (B): Sample of 8 BEA regions with sectoral breakdown. Percent responses of 1-year ahead GDP to a one-standard-deviation shock to the factor. Bars indicate the 90th percentiles. Since the BEA stopped updating GDP by state before 1997, we map the previous SIC to the current NAICS. Specifically, the SIC "communications" sector is connected to "information" under the NAICS; the SIC "service" is the sum of "professional and business services," "management of companies and enterprises," "educational service, health care, and social assistance," and "arts, entertainment, recreation, accommodation, and food services"; other sectors are connected to the sectors with the same labels in the SIC and the NAICS.

4.4.2 The U.S.

Next, we explore sectoral data within the U.S. Using annual GDP data compiled by the Bureau of Economic Analysis (BEA) since 1977 (with quarterly data available from 2005:Q1

onward), we employ a panel LP approach outlined in equation (5) covering the period from 1986 to 2022. The control variables include U.S. aggregate GDP growth and the same global variables utilized in the cross-country analysis. The fragmentation shocks, aggregated annually, serve as the central variable of interest.

Panel (B) of Figure 7 illustrates the responses at impact to a fragmentation shock in U.S. sectoral GDP. Our focus is on the ten major private sectors and the government sector at the 2-digit level of the SIC within regional GDP. The figure highlights the concentrated adverse effects of fragmentation in specific sectors, including manufacturing, durable goods, transportation, and wholesale, likely attributed to the heightened exposure of these sectors to global economic activities.

5 Geopolitical Bloc Fragmentation

Given our previous results, a natural question arises: Is the global trend of fragmentation distributed evenly or unevenly across different regions of the world? For instance, an extreme consequence of fragmentation would be the division of the world into separate economic blocs, each with its own dynamics.

While the world economy has not yet fully divided into these separate blocs, we can measure the extent to which fragmentation between and within blocs is already significant. Does the degree of fragmentation within different geopolitical blocs affect the bloc's aggregate dynamics? Does fragmentation in different regions impact the global economy differently? To answer these questions, we explore fragmentation within geopolitical blocs and examine the potentially heterogeneous effects of each bloc's fragmentation on the global economy.

5.1 Measuring geopolitical bloc fragmentation

We expand our baseline DFM by considering three geopolitical blocs: the U.S.-EU bloc, the China-Russia bloc, and the Others bloc. For each bloc, we collect eight empirical indicators reflecting geopolitical fragmentation and are chosen based on their availability: trade openness, FDI ratio, financial flow ratio, trade restrictions, capital control measures, sanctions, geopolitical risk index, and the UNGA kappa score. The data used for estimation are detailed in Appendix C.4.

Specifically, we express equation (2) for each of these three blocs. With the exception of the treatment of the factor, all other aspects are treated symmetrically. We utilize the same priors as those employed in our baseline case. When considering the factor for the global bloc,

we utilize a hierarchical structure, expressing it as weighted averages of the local factors:

$$f_t = \sum_{j \in \{\text{U.S.-EU,CHN-RUS, Others}\}} w_j f_t^{(j)}, \tag{7}$$

where f_t represents the global fragmentation factor, while $f_t^{(j)}$ denotes the local fragmentation bloc factor in bloc j. We estimate the entire specification jointly, including the weights w_j. We impose the prior $w_j \sim \mathcal{N}\left(\frac{1}{3}, \frac{1}{100}\right)$ for the weights. Appendix B reports the comprehensive details of the extended model.

Figure 8: Estimated geopolitical bloc fragmentation indices

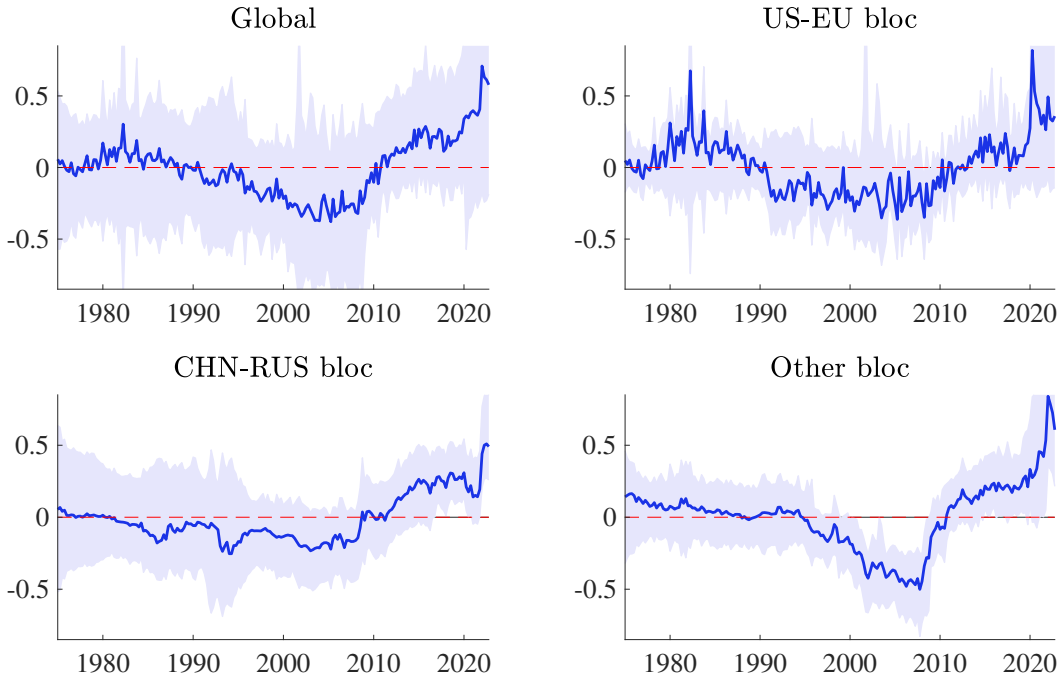

Notes: We present the posterior median-smoothed estimates of $f_t^{(j)}$ accompanied by 90% credible intervals where $j = \{\text{U.S.-EU, CHN-RUS, Others}\}$. The global index is obtained by $f_t = \sum_{j=1}^{3} w_j f_t^{(j)}$.

Figure 8 displays the estimated bloc fragmentation indices. These indices share broad patterns with the global index, including the tendency toward globalization before the 2007-2008 financial crisis and fragmentation afterward. However, a closer look reveals several notable differences across geopolitical blocs.

In the U.S.-EU bloc, a globalization trend started in the 1980s and further advanced in the early 1990s. The timing corresponds to the era of greater trade and capital flows under the floating exchange rate regime, particularly among advanced economies. The advance of globalization in the early 1990s picks up at the end of the Cold War. This result is intuitive as the U.S. and the EU were among the first economies to embrace liberalization policies in the late 1970s and early 1980s.

The globalization of the other blocs lagged and started around the mid-1990s when trade liberalization gained momentum in large emerging economies. The movement was underpinned by regional trade agreements, such as NAFTA and Mercosur, as well as global institutions, such as the WTO. The trend was reinforced by growing trade and increasing financial flows into emerging economies, but the trend largely reverted after the 2007-2008 financial crisis.

The dynamics of the China-Russia bloc's factor are affected by individual events, such as the dissolution of the USSR in 1991 and China's move toward a market economy, including the participation in the WTO in 2001 and the gradual deregulation of capital flows. The pronounced width of the credible interval for the China-Russia bloc fragmentation index until the mid-1990s is a reflection of the limited availability of most empirical indicators. The dynamics of the Other bloc's factor resemble those depicted in Figure 2, possibly attributable to similarities in the empirical indicators compared to those corresponding to global indicators.

Finally, notice that the estimated global fragmentation index closely mirrors the pattern illustrated in Figure 2, with a correlation of around 0.87. This observation is not entirely unexpected, given our earlier insights from Figure 3, where the robust estimation of the global fragmentation index remained consistent across various empirical indicators. However, there is a discernible contrast in the smoothness of the factor. While the overarching low-frequency dynamics align, the global index exhibits slight fluctuations due to its reliance on the U.S.-EU bloc fragmentation index, which displays more variability. This difference results in the correlation dipping just below 0.9.

5.2 Assessing the causal effects of geopolitical bloc fragmentation

Next, we explore the ramifications of bloc fragmentation dynamics for global and regional economies. We employ sign restrictions to identify bloc fragmentation shocks.

Initially, we estimate a VAR model encompassing the following global and bloc variables:

$$Y_t' = \begin{bmatrix} f_t^{\text{U.S.-EU}} - f_t, & f_t^{\text{CHN-RUS}} - f_t, & f_t^{\text{Others}} - f_t, & f_t, & \text{VIX}_t, \\ \ln(\text{S\&P}_t), & \ln(\text{WTI}_t), & \text{U.S. Treasury}_t, & \text{NFCI}_t, & \ln(\text{World GDP}_t) \end{bmatrix}. \quad (8)$$

Here, the first three entries represent the differentials of local and global fragmentation factors. Local fragmentation shocks are defined as those that increase (decrease) global fragmentation and render the own bloc more (less) fragmented than other blocs. This is achieved by imposing

the following sign restrictions:

$$\begin{bmatrix} u_t^{\text{U.S.-EU}} - u_t^{\text{Global}} \\ u_t^{\text{CHN-RUS}} - u_t^{\text{Global}} \\ u_t^{\text{Others}} - u_t^{\text{Global}} \\ u_t^{\text{Global}} \\ \vdots \end{bmatrix} = \begin{bmatrix} + & ? & ? & \cdots \\ ? & + & ? & \cdots \\ ? & ? & + & \cdots \\ + & + & + & \cdots \\ \vdots & \vdots & \vdots & \ddots \end{bmatrix} \begin{bmatrix} \varepsilon_t^{\text{U.S.-EU}} \\ \varepsilon_t^{\text{CHN-RUS}} \\ \varepsilon_t^{\text{Others}} \\ \vdots \end{bmatrix}, \tag{9}$$

where $u_t^{(j)}$ is the reduced-form residuals from the VAR and $\varepsilon_t^{(j)}$ is the bloc-driven fragmentation shocks. The sign restrictions are imposed for four quarters after the shock and reflect standard intuition. For example, more fragmentation between the U.S. and the EU leads to larger reduced-form VAR residuals from the U.S.-EU bloc than in the world as a whole. This reflects the fact that the joint aggregate dynamics of the U.S. and the EU are more affected by fragmentation within their own bloc than by fragmentation in other blocs.

Then, the identified local fragmentation shocks are added to the baseline panel VAR.[4] Each bloc's shock is included in the VAR separately. The local fragmentation shock is ordered first in the Cholesky decomposition when calculating the IRFs.

Figure 9 presents the results. The U.S.-EU and Others fragmentation shocks have immediate adverse effects on the global economy. In contrast, the China-Russia fragmentation shocks initially have subtle positive impacts and, then, persistent negative effects in later years. The delayed impacts of the China-Russia shocks may suggest that the advance of China into the global market increased competition and partly substituted the presence of other countries. Similarly, there is most likely a trade relocation in the U.S. from China to other emerging economies following the U.S.-China trade war in 2018-19.

In Appendix D.3, we present the IRFs of countries within each bloc (or all blocs) to various fragmentation shocks. We observe that the U.S.-EU and other blocs exhibit similar responses, aligning with those of the global economy. In contrast, the responses of the China-Russia bloc are ambiguous, lacking clear patterns, indicating the unique dynamics of their economies.

[4]The resulting VAR has 12 variables:

$$Y_{it}' = \begin{bmatrix} \varepsilon_t^{(j)}, & f_t, & \text{VIX}_t, & \ln(\text{S\&P}_t), & \ln(\text{WTI}_t), & \text{U.S. Treasury}_t, \\ \text{NFCI}_t, & \ln(\text{World GDP}_t), & \ln(\text{SP}_{it}), & \text{IP}_{it}, & \ln(\text{I}_{it}), & \ln(\text{GDP}_{it}) \end{bmatrix}$$

Figure 9: Economic impact of bloc-driven fragmentation: SVAR

US-EU Shock (1st row); CHN-RUS Shock (2nd row); Others Shock (3rd row)

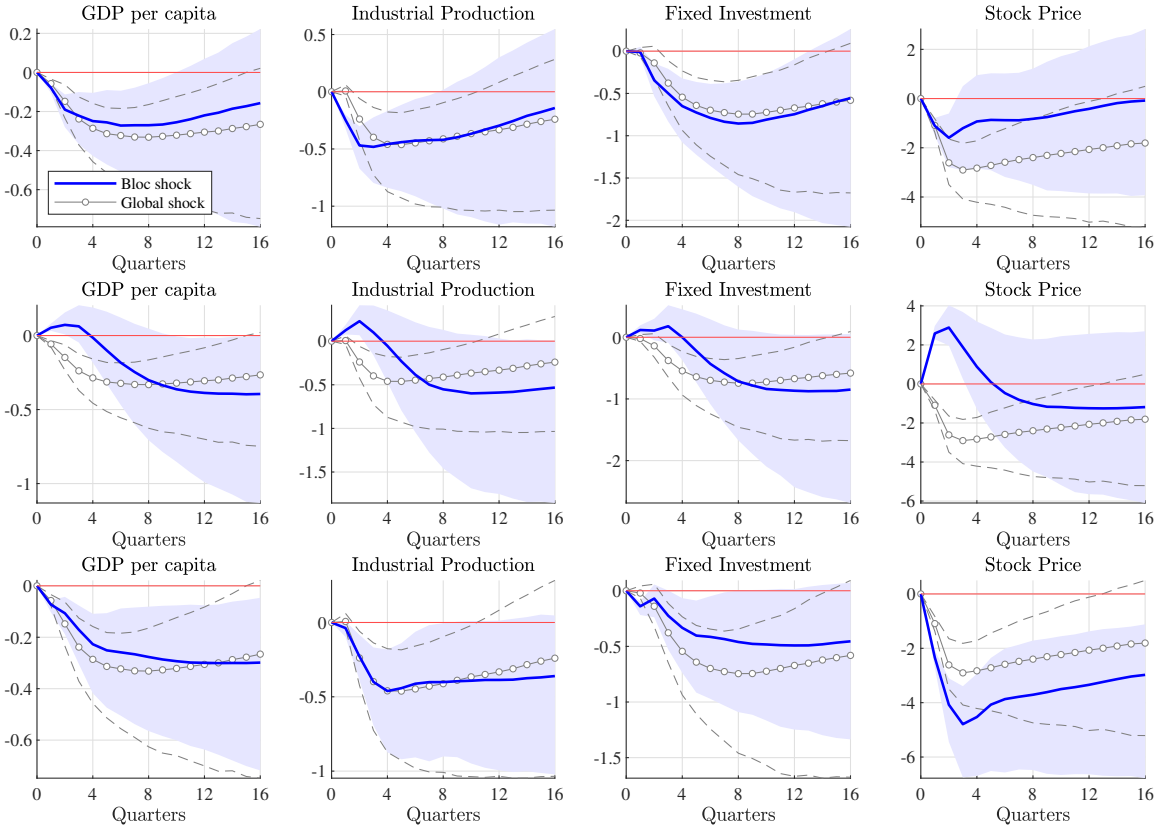

Notes: Sample of AEs and EMs. Percent responses to a one-standard-deviation shock. Shaded areas indicate the 90th percentiles where standard errors are clustered by time. The horizon of sign restrictions is set to 4 quarters. The IRFs to the baseline global fragmentation shock (Cholesky decomposition) are shown in gray as a reference.

6 Conclusions

After decades of global economic integration, recent trends point to a shift toward fragmentation. We offer a measure of geopolitical fragmentation, drawn from diverse empirical indicators, to precisely assess the current state and contribute to understanding its causal effects on the global economy. Leveraging a widely used method extended for maximum flexibility, our estimated DFM with time-varying parameters and stochastic volatility captures the evolving dynamics of global fragmentation.

Our analysis, employing SVAR and LP, reveals the causal relationships between changes in fragmentation and their impacts on the global economy. We find that heightened fragmentation, indicated by a positive one-standard-deviation shock to the fragmentation index, detrimentally affects the global economy, with emerging economies disproportionately affected compared to advanced ones. Importantly, we uncover an inherent asymmetry: while fragmentation immediately impairs the global economy, the benefits of reduced fragmentation, often

associated with positive aspects of globalization, unfold gradually over time. Additionally, our examination of sectors within OECD economies highlights the adverse repercussions of fragmentation for industries intricately connected to global markets, including manufacturing, construction, finance, and wholesale and retail trade.

References

Acemoglu, D., Gancia, G., and Zilibotti, F. (2015). Offshoring and directed technical change. *American Economic Journal: Macroeconomics*, 7:84–122.

Ahir, H., Bloom, N., and Furceri, D. (2022). The World Uncertainty Index. Working Paper 29763, National Bureau of Economic Research.

Aiyar, S., Chen, J., Ebeke, C., Ebeke, C. H., Garcia-Saltos, R., Gudmundsson, T., Ilyina, A., Kangur, A., Kunaratskul, T., Rodriguez, M. S. L., et al. (2023a). *Geo-economic Fragmentation and the Future of Multilateralism*. International Monetary Fund.

Aiyar, S., Presbitero, A., and Ruta, M. (2023b). *Geoeconomic Fragmentation: The Economic Risks from a Fractured World Economy*. CEPR Press.

Amiti, M., Redding, S. J., and Weinstein, D. E. (2020). Who's paying for the US tariffs? A longer-term perspective. *AEA Papers and Proceedings*, 110:541–546.

Antrás, P. (2020). De-globalisation? Global value chains in the post-COVID-19 age. Mimeo.

Arias, J. E., Fernández-Villaverde, J., Rubio-Ramírez, J. F., and Shin, M. (2023). The causal effects of lockdown policies on health and macroeconomic outcomes. *American Economic Journal: Macroeconomics*, 15(3):287–319.

Aruoba, S. B., Diebold, F. X., and Scotti, C. (2009). Real-time measurement of business conditions. *Journal of Business and Economic Statistics*, 27(4):417–427.

Attinasi, M. G., Boeckelmann, L., and Meunier, B. (2023). The economic costs of supply chain decoupling. ECB Working Paper No. 2023/2839.

Bai, X., Fernández-Villaverde, J., Li, Y., and Zanetti, F. (2024). The causal effects of global supply chain disruptions on macroeconomic outcomes: Evidence and theory. Manuscript.

Baker, M. and Wurgler, J. (2007). Investor sentiment in the stock market. *Journal of Economic Perspectives*, 21(2):129–152.

Baker, S. R., Bloom, N., and Davis, S. J. (2016). Measuring economic policy uncertainty. *Quarterly Journal of Economics*, 131(4):1593–1636.

Blanga-Gubbay, M. and Rubinova, S. (2023). Is the global economy fragmenting? World Trade Organization Staff Working Paper 2023-10.

Bloom, N., Bunn, P., Chen, S., Mizen, P., Smietanka, P., and Thwaites, G. (2019). The impact of Brexit on UK firms. NBER Working Paper No. 26218.

Bloom, N., Davis, S., and Baker, S. (2015). Immigration fears and policy uncertainty. VOXEU Column, 15 December, 2015.

Bolhuis, M. A., Chen, J., and Kett, B. (2023). Fragmentation in global trade: Accounting for commodities. IMF Working Paper WP/23/73, International Monetary Fund.

Bustos, P. (2011). Trade liberalization, exports, and technology upgrading: Evidence on the impact of MERCOSUR on Argentinian firms. *American Economic Review*, 101:304–340.

Caldara, D. and Iacoviello, M. (2022). Measuring geopolitical risk. *American Economic Review*, 112(4):1194–1225.

Caldara, D., Iacoviello, M., Molligo, P., Prestipino, A., and Raffo, A. (2020). The economic effects of trade policy uncertainty. *Journal of Monetary Economics*, 109:38–59.

Campos, R. G., Estefania-Flores, J., Furceri, D., and Timin, J. (2023). Geopolitical fragmentation and trade. *Journal of Comparative Economics*, 51(4):1289–1315.

Carter, C. K. and Kohn, R. (1994). On Gibbs sampling for state space models. *Biometrika*, 81(3):541–553.

Cerdeiro, D. A., Eugster, J., Mano, R. C., Muir, D., and Peiris, S. J. (2021). Sizing up the effects of technological decoupling. IMF Working Paper, WP/21/69.

Clayton, C., Maggiori, M., and Schreger, J. (2024). A theory of economic coercion and fragmentation. Manuscript.

Dang, T. H.-N., Nguyen, C. P., Lee, G. S., Nguyen, B. Q., and Le, T. T. (2023). Measuring the energy-related uncertainty index. *Energy Economics*, 124(106817).

Del Negro, M. and Otrok, C. (2008). Dynamic factor models with time-varying parameters: Measuring changes in international business cycles. *Federal Reserve Bank of New York Staff Reports no. 326*.

Del Negro, M. and Schorfheide, F. (2011). Bayesian macroeconometrics. In Geweke, J., Koop, G., and van Dijk, H., editors, *The Oxford Handbook of Bayesian Econometrics*, pages 293–389. Oxford University Press.

Durbin, J. and Koopman, S. J. (2001). *Time Series Analysis by State Space Methods*. Oxford University Press.

Erten, B., Korinek, A., and Ocampo, J. A. (2021). Capital controls: Theory and evidence. *Journal of Economic Literature*, 59(1):45–89.

Fajgelbaum, P. D., Goldberg, P. K., Kennedy, P. J., and Khandelwal, A. K. (2019). Return to protectionism. *Quarterly Journal of Economics*, 135:1–55.

Fajgelbaum, P. D. and Khandelwal, A. K. (2022). The economic impacts of the US–China trade war. *Annual Review of Economics*, 14:205–228.

Feenstra, R. C. (2006). New evidence on the gains from trade. *Review of World Economics / Weltwirtschaftliches Archiv*, 142(4):617–641.

Felbermayr, G., Kirilakha, A., Syropoulos, C., Yalcin, E., and Yotov, Y. V. (2020). The global sanctions data base. *European Economic Review*, 129:103561.

Fernández, A., Klein, M. W., Rebucci, A., Schindler, M., and Uribe, M. (2016). Capital control measures: A new dataset. *IMF Economic Review*, 64:548–574.

Flaaen, A. and Pierce, J. (2019). Disentangling the effects of the 2018-2019 tariffs on a globally connected U.S. manufacturing sector. Finance and Economics Discussion Series 2019-086, Federal Reserve Board.

Frankel, J. A. and Romer, D. H. (1999). Does trade cause growth? *American Economic Review*, 89(3):379–399.

Geweke, J. (1977). The dynamic factor analysis of economic time series. In Aigner, D. J. and Goldberger, A. S., editors, *Latent Variables in Socio-Economic Models*, chapter 19. North Holland, Amsterdam.

Geweke, J. and Zhou, G. (1996). Measuring the pricing error of the arbitrage pricing theory. *Review of Financial Studies*, 9(2):557–587.

Gilchrist, S. and Zakrajšek, E. (2012). Credit spreads and business cycle fluctuations. *American Economic Review*, 102(4):1692–1720.

Glennon, B. (2024). How do restrictions on high-skilled immigration affect offshoring? Evidence from the H-1B program. *Management Science*, 70:907–930.

Góes, C. and Bekkers, E. (2022). The impact of geopolitical conflicts on trade, growth, and innovation. World Trade Organization, Staff Working Paper ERSD-2022-09.

Goldberg, P. K. and Reed, T. (2023). Is the global economy deglobalizing? And if so, why? And what is next? NBER Working Paper No. 31115.

Gopinath, G. (2023). Cold War II? Preserving economic cooperation amid geoeconomic fragmentation. Plenary Speech at the 20th World Congress of the International Economic Association, Colombia, December 11, 2023.

Gopinath, G., Gourinchas, P.-O., Presbitero, A., and Topalova, P. (2024). Changing global linkages: A new Cold War? IMF Working Paper No. 2024/076.

Häge, F. M. (2017). Chance-corrected measures of foreign policy similarity (FPSIM Version 2). Harvard Dataverse, V2.

Hakobyan, S., Meleshchuk, S., and Zymek, R. (2023). Divided we fall: Differential exposure to geopolitical fragmentation in trade. IMF Working Paper No. 2023/270.

Handley, K., Kamal, F., and Monarch, R. (2020). Rising import tariffs, falling export growth: When modern supply chains meet old-style protectionism. NBER Working Paper No. 26611.

Javorcik, B. S., Kitzmueller, L., Schweiger, H., and Yıldırım, M. A. (2024). Economic costs of friendshoring. *The World Economy*, 00:1–38.

Jurado, K., Ludvigson, S. C., and Ng, S. (2015). Measuring uncertainty. *American Economic Review*, 105(3):1177–1216.

Kim, S., Shephard, N., and Chib, S. (1998). Stochastic volatility: Likelihood inference and comparison with ARCH models. *Review of Economic Studies*, 65(3):361–393.

LaBelle, J., Martinez-Zarzoso, I., Santacreu, A. M., and Yotov, Y. (2023). Cross-border patenting, globalization, and development. Federal Reserve Bank of St. Louis Working Paper 2023-031.

Melitz, M. J. and Trefler, D. (2012). Gains from trade when firms matter. *Journal of Economic Perspectives*, 26(2):91–118.

Mertens, K. and Ravn, M. O. (2013). The dynamic effects of personal and corporate income tax changes in the United States. *American Economic Review*, 103(4):1212–1247.

Montiel Olea, J. L. and Plagborg-Møller, M. (2021). Local projection inference is simpler and more robust than you think. *Econometrica*, 89(4):1789–1823.

Obstfeld, M. (1994). Risk-taking, global diversification, and growth. *American Economic Review*, 84:1310–1329.

Otrok, C. and Whiteman, C. H. (1998). Bayesian leading indicators: Measuring and predicting economic conditions in Iowa. *International Economic Review*, 39(4):997–1014.

Plagborg-Møller, M. and Wolf, C. K. (2021). Local projection and VARs estimate the same impulse. *Econometrica*, 89(2):955–980.

Sampson, T. (2017). Brexit: The economics of international disintegration. *Journal of Economic Perspectives*, 31:163–184.

Sargent, T. J. and Sims, C. A. (1977). Business cycle modeling without pretending to have too much a priori economic theory. In *New Methods in Business Cycle Research*. FRB Minneapolis, Minneapolis.

Shapiro, A. H., Sudhof, M., and Wilson, D. J. (2022). Measuring news sentiment. *Journal of Econometrics*, 228(2):221–243.

Stock, J. H. and Watson, M. W. (1989). New indices of coincident and leading economic indicators. In Blanchard, O. J. and Fischer, S., editors, *NBER Macroeconomics Annual 1989*, volume 4, pages 351–394. MIT Press, Cambridge.

Utar, H., Ruiz, L. B. T., and Zurita, A. C. (2023). The US-China trade war and the relocation of global value chains to Mexico. CESifo Working Paper No. 10638.

Wu, J. C. and Xia, F. D. (2016). Measuring the macroeconomic impact of monetary policy at the zero lower bound. *Journal of Money, Credit and Banking*, 48(2-3):253–291.

Appendix

A Estimation of the Dynamic Factor Model

The DFM with time-varying parameters is specified as follows:

$$
\begin{aligned}
y_{i,t} &= a_{i,t} + b_{i,t} f_t + u_{i,t}, \\
a_{i,t} &= a_{i,0} + a_{i,1} t, \\
f_t &= \phi_{f,1} f_{t-1} + ... + \phi_{f,p} f_{t-p} + \sigma_{f,t} \epsilon_{f,t}, \quad \epsilon_{f,t} \sim \mathcal{N}(0,1), \\
b_{i,t} &= b_{i,t-1} + \sigma_{b_i} \epsilon_{b_i,t}, \quad \epsilon_{b_i,t} \sim \mathcal{N}(0,1), \\
u_{i,t} &= \phi_{u_i,1} u_{i,t-1} + ... + \phi_{u_i,q} u_{i,t-q} + \sigma_{u_i,t} \epsilon_{u_i,t}, \quad \epsilon_{u_i,t} \sim \mathcal{N}(0,1), \\
h_{j,t} &= h_{j,t-1} + \sigma_{h_j} \epsilon_{h_j,t}, \quad \sigma_{j,t} = \sigma_j \exp(h_{j,t}), \quad \epsilon_{h_j,t} \sim \mathcal{N}(0,1),
\end{aligned} \tag{A-1}
$$

where $i \in \{1, ..., N\}$ and $j \in \{f, u_1, ..., u_N\}$. To simplify the explanation, we gather the parameters in (A-1) as:

$$
\begin{aligned}
a_0 &= \begin{bmatrix} a_{0,1} \\ \vdots \\ a_{0,N} \end{bmatrix}, \quad a_1 = \begin{bmatrix} a_{1,1} \\ \vdots \\ a_{1,N} \end{bmatrix}, \quad b_t = \begin{bmatrix} b_{1,t} \\ \vdots \\ b_{N,t} \end{bmatrix}, \quad \sigma_b = \begin{bmatrix} \sigma_{b_1} \\ \vdots \\ \sigma_{b_N} \end{bmatrix}, \quad \phi_f = \begin{bmatrix} \phi_{f,1} \\ \vdots \\ \phi_{f,p} \end{bmatrix}, \\
\phi_{u_i} &= \begin{bmatrix} \phi_{u_i,1} \\ \vdots \\ \phi_{u_i,q} \end{bmatrix}, \quad \phi_u = \begin{bmatrix} \phi_{u_1} \\ \vdots \\ \phi_{u_N} \end{bmatrix}, \quad \sigma_u = \begin{bmatrix} \sigma_{u_1} \\ \vdots \\ \sigma_{u_N} \end{bmatrix}, \quad \sigma_{h_u} = \begin{bmatrix} \sigma_{h_{u_1}} \\ \vdots \\ \sigma_{h_{u_N}} \end{bmatrix}.
\end{aligned} \tag{A-2}
$$

The model unknowns can be categorized into three sets:

$$
\Theta_f = \{f^T, \phi_f, \sigma_f, h_f^T\}, \quad \Theta_b = \{b^T, \sigma_b\}, \quad \Theta_u = \{a_0, a_1, \phi_u, \sigma_u, h_u^T\}.
$$

A.1 Gibbs sampler

We use the Gibbs sampler to estimate the model unknowns. For the k-th iteration:

(G1) Appendix A.2: Run Kalman filter and smoother using the algorithm to update $\Theta_f^{(k)}$ conditional on $\Theta_f^{(k-1)}, \Theta_b^{(k-1)}, \Theta_u^{(k-1)}$.

(G2) Appendix A.3: Run Kalman filter and smoother using the algorithm to update $\Theta_b^{(k)}$ conditional on $\Theta_f^{(k)}, \Theta_b^{(k-1)}, \Theta_u^{(k-1)}$.

(G3) Appendix A.4: Update the remaining parameters, including ones associated with the serially correlated innovation $\Theta_u^{(k)}$ conditional on $\Theta_f^{(k)}, \Theta_b^{(k)}, \Theta_u^{(k-1)}$.

A.2 Updating the factor and the associated parameters: $\Theta_f^{(k)}$

For ease of exposition, we omit the superscript (k). We re-express (A-1) as:

$$\begin{aligned}
\tilde{y}_{i,t} &= \tilde{a}_{i,t} + \tilde{b}_{i,t}\tilde{f}_t + \sigma_{u_i,t}\epsilon_{u_i,t}, \\
\tilde{y}_{i,t} &= (y_{i,t} - \phi_{u_i,1}y_{i,t-1} ... - \phi_{u_i,q}y_{i,t-q}), \\
\tilde{a}_{i,t} &= a_{i,0}(1 - \phi_{u_i,1} ... - \phi_{u_i,q}) + a_{i,1}(t - \phi_{u_i,1}(t-1) ... - \phi_{u_i,q}(t-q)), \\
\tilde{b}_{i,t} &= \begin{bmatrix} b_{i,t} & -b_{i,t-1}\phi_{u_i,1} & \dots & -b_{i,t-q}\phi_{u_i,q} \end{bmatrix}.
\end{aligned} \tag{A-3}$$

Note that (A-4) implies the following state-space representation:

$$\begin{aligned}
\begin{bmatrix} \tilde{y}_{1,t} \\ \vdots \\ \tilde{y}_{N,t} \end{bmatrix} &= \begin{bmatrix} \tilde{a}_{1,t} \\ \vdots \\ \tilde{a}_{N,t} \end{bmatrix} + \begin{bmatrix} \tilde{b}_{1,t} \\ \vdots \\ \tilde{b}_{N,t} \end{bmatrix} \cdot \begin{bmatrix} f_t \\ f_{t-1} \\ \vdots \\ f_{t-q} \end{bmatrix} + \begin{bmatrix} \sigma_{u_1,t}\epsilon_{u_1,t} \\ \vdots \\ \sigma_{u_N,t}\epsilon_{u_N,t} \end{bmatrix}, \\
\begin{bmatrix} f_t \\ f_{t-1} \\ \vdots \\ f_{t-q} \end{bmatrix} &= \begin{bmatrix} \phi_{f,1} & \dots & \phi_{f,p} & \dots \\ 1 & \dots & 0 & \dots \\ 0 & \ddots & \vdots & \dots \\ \dots & 0 & 1 & \dots \end{bmatrix} \begin{bmatrix} f_{t-1} \\ f_{t-2} \\ \vdots \\ f_{t-q-1} \end{bmatrix} + \begin{bmatrix} \sigma_{f,t}\epsilon_{f,t} \\ 0 \\ \vdots \\ 0 \end{bmatrix}.
\end{aligned} \tag{A-4}$$

Based on the state-space representation in (A-4), we draw f^T based on the forward filtering and backward smoothing algorithm explained in Appendix A.5. Conditional on the drawn f^T, we draw $\{\phi_f, \sigma_f, h_f^T\}$ based on the procedure described in Appendix A.6.

A.3 Updating the factor loading and the associated parameter: $\Theta_b^{(k)}$

For ease of exposition, we omit the superscript (k).

For each $i \in \{1, ..., N\}$, we re-express (A-1) as

$$
\begin{aligned}
\hat{y}_{i,t} &= \hat{a}_{i,t} + \hat{f}_t \hat{b}_{i,t} + \sigma_{u_i,t} \epsilon_{u_i,t}, \\
\hat{y}_{i,t} &= (y_{i,t} - \phi_{u_i,1} y_{i,t-1} ... - \phi_{u_i,q} y_{i,t-q}), \\
\tilde{a}_{i,t} &= a_{i,0}(1 - \phi_{u_i,1} ... - \phi_{u_i,q}) + a_{i,1}(t - \phi_{u_i,1}(t-1) ... - \phi_{u_i,q}(t-q)), \\
\hat{f}_t &= \begin{bmatrix} f_t & -f_{t-1}\phi_{u_i,1} & \dots & -f_{t-q}\phi_{u_i,q} \end{bmatrix}, \\
\hat{b}_{i,t} &= \begin{bmatrix} b_{i,t} \\ b_{i,t-1} \\ \vdots \\ b_{i,t-q} \end{bmatrix} = \begin{bmatrix} 1 & \dots & 0 & \dots \\ 1 & \dots & 0 & \dots \\ 0 & \ddots & \vdots & \dots \\ \dots & 0 & 1 & \dots \end{bmatrix} \begin{bmatrix} b_{i,t-1} \\ b_{i,t-2} \\ \vdots \\ b_{i,t-q-1} \end{bmatrix} + \begin{bmatrix} \sigma_{b_i} \epsilon_{b_i,t} \\ 0 \\ \vdots \\ 0 \end{bmatrix}.
\end{aligned} \tag{A-5}
$$

Based on the state-space representation in (A-5), we draw b_i^T based on the forward filtering and backward smoothing algorithm explained in Appendix A.5. Conditional on the drawn b_i^T, we draw σ_{b_i} based on the procedure described in Appendix A.6.

A.4 Updating the remaining parameters: $\Theta_u^{(k)}$

For ease of exposition, we omit the superscript (k). First, conditional on $\{\phi_u, \sigma_u, h_u^T\}$, we re-express (A-1) as:

$$
\bar{y}_{i,t} = a_i \bar{x}_{i,t} + \sigma_{u_i} \epsilon_{u_i,t}, \tag{A-6}
$$

where:

$$
\bar{y}_{i,t} = \frac{\hat{y}_{i,t} - \hat{f}_t \hat{b}_{i,t}}{\exp(h_{u_i,t})}, \quad \bar{x}_{i,t} = \begin{bmatrix} \frac{1 - \phi_{u_i,1} ... - \phi_{u_i,q}}{\exp(h_{u_i,t})}, & \frac{t - \phi_{u_i,1}(t-1) ... - \phi_{u_i,q}(t-q)}{\exp(h_{u_i,t})} \end{bmatrix},
$$

and $\hat{y}_{i,t}$, $\hat{f}_t$, and $\hat{b}_{i,t}$ are provided in (A-5). We draw a_i based on the procedure described in Appendix A.6. Second, conditional on the updated a, we re-express (A-1) as

$$
u_{i,t} = y_{i,t} - a_{i,t} - b_{i,t} f_t \tag{A-7}
$$

and update the associated parameters and stochastic volatilities $\{\phi_u, \sigma_u, h_u^T\}$ of the serially correlated errors based on the procedure described in Appendix A.6.

A.5 Forward filtering and backward smoothing algorithm

To illustrate the forward filtering and backward smoothing algorithm by Carter and Kohn (1994), we will use a generic expression for the state-space model:

$$\begin{aligned} o_t &= A + Z_t s_t + \eta_t, \quad \eta_t \sim \mathcal{N}(0, \Omega_t), \\ s_t &= \Phi s_{t-1} + \varepsilon_t, \quad \varepsilon_t \sim \mathcal{N}(0, \Sigma_t). \end{aligned}$$

We summarize the Kalman filter as described in Durbin and Koopman (2001). Suppose that the distribution of:

$$s_{t-1}|y^{t-1} \sim \mathcal{N}(s_{t-1|t-1}, P_{t-1|t-1}).$$

Then, the Kalman filter forecasting and updating equations take the form:

$$\begin{aligned} s_{t|t-1} &= \Phi s_{t-1|t-1} \\ P_{t|t-1} &= \Phi P_{t-1|t-1}\Phi' + \Sigma_t \\ s_{t|t} &= s_{t|t-1} + (Z_t P_{t|t-1})'(Z_t P_{t|t-1} Z_t')^{-1}\left(o_t - A - Z_t s_{t|t-1}\right) \\ P_{t|t} &= P_{t|t-1} - (Z_t P_{t|t-1})'(Z_t P_{t|t-1} Z_t')^{-1}(Z_t P_{t|t-1}). \end{aligned}$$

In turn,

$$s_t|o^t \sim \mathcal{N}(s_{t|t}, P_{t|t}).$$

The backward smoothing algorithm developed by Carter and Kohn (1994) is applied to generate draws from the distributions $s_\tau$recursively$|s_{\tau+1}, ..., s_T, o^T$ (ignoring dependency on model unknowns) for $\tau = T-1, T-2, \ldots, 1$. The last elements of the Kalman filter recursion provide the initialization for the simulation smoother:

$$\begin{aligned} s_{\tau|\tau+1} &= s_{\tau|\tau} + P_{\tau|\tau}\Phi' P_{\tau+1|t}^{-1}\left(s_{\tau+1} - \Phi s_{\tau|\tau}\right) \\ P_{\tau|\tau+1} &= P_{\tau|\tau} - P_{\tau|\tau}\Phi' P_{\tau+1|\tau}^{-1}\Phi P_{\tau|\tau} \\ \text{draw } s_\tau &\sim N(s_{\tau|\tau+1}, P_{\tau|\tau+1}), \qquad \tau = T-1, T-2, ..., 1. \end{aligned}$$

A.6 Drawing persistence, variance, and stochastic volatility of the autoregressive model

To illustrate the procedure, we will use a generic expression for the autoregressive model. To simplify, we assume an AR(1) model with stochastic volatility as described in (A-8)

$$x_t = \rho_x x_{t-1} + \sigma_x \exp(h_t)\epsilon_{x,t}, \quad \epsilon_{x,t} \sim \mathcal{N}(0,1). \tag{A-8}$$

Drawing ρ_x. In order to obtain posterior for ρ_x, we assume that for $t \leq 0$, $h_t = 0$. Under

this assumption, x_0 is generated from a stationary distribution. Express the unconditional distribution as

$$x_0 \sim N(0, \Sigma_{x_0}),$$

where $\Sigma_{x_0} = \frac{1}{(1-\rho_x^2)}$. From (A-8), we get $var(x_1) = \rho_x^2 var(x_0) + \exp(2h_1) = S_{x_0}$, where $S_{x_0} = \rho_x^2 \Sigma_{x_0} + \exp(2h_1)$.

We write the conditional likelihood of the first factor element as:

$$L(x_1|h_1, \rho_x) = \frac{1}{\sqrt{2\pi S_{x0}}} \exp\left\{-\frac{1}{2S_{x0}} x_1^2\right\}, \tag{A-9}$$

and the remaining $T-1$ elements as:

$$\begin{aligned} L(x_2, ..., x_T|h_{1:T}, \rho_x) &= \prod_{t=2}^{T} \frac{1}{\sqrt{2\pi \exp(2h_t)}} \exp\left\{-\frac{1}{2}(\frac{x_t - \rho_x x_{t-1}}{\exp(h_t)})'(\frac{x_t - \rho_x x_{t-1}}{\exp(h_t)})\right\} \\ &\propto \exp\left\{\frac{1}{2}(e_0 - E_0\rho_x)'(e_0 - E_0\rho_x)\right\} \end{aligned} \tag{A-10}$$

where:

$$e_0 = \begin{bmatrix} \frac{x_2}{\exp(h_2)} \\ \vdots \\ \frac{x_T}{\exp(h_T)} \end{bmatrix}, \quad E_0 = \begin{bmatrix} \frac{x_1}{\exp(h_2)} \\ \vdots \\ \frac{x_{T-1}}{\exp(h_T)} \end{bmatrix}.$$

We use

$$\rho_x \sim N(V_{\rho_x}^{-1}(\bar{V}_{\rho_x}\bar{\rho}_x + E_0'e_0), V_{\rho_x}^{-1})$$

as a proposal distribution, where $V_{\rho_x} = \bar{V}_{\rho_x} + E_0'E_0$. In a Metropolis-Hastings step, we accept the draw ρ_x generated from the proposal distribution with probability

$$\min\left\{\frac{L(x_1|h_1, \rho_x^{(k)})}{L(x_1|h_1, \rho_x^{(k-1)})}, 1\right\}.$$

Drawing σ_x^2. The posterior for σ_x^2 is given by:

$$\sigma_x^2 \sim \mathcal{IG}\left(\frac{\bar{T}+T}{2}, \bar{v} + (e_0 - E_0\rho_x)'(e_0 - E_0\rho_x)\right).$$

Drawing h^T. The last step of the Gibbs sampler draws the stochastic volatilities conditional

on all other parameters. Define γ_t such that:

$$\gamma_t = \left(\frac{x_t - \rho_x x_{t-1}}{\sigma_x} \right) = \exp(h_t)\epsilon_{x,t}.$$

Taking squares and then logs of z_t produces,

$$z_t^* = 2h_t + u_t^* \tag{A-11}$$

$$h_t = \rho_h h_{t-1} + \sigma_h \varepsilon_t. \tag{A-12}$$

where $z_t^* = log(\gamma_t^2 + 0.001)$ and $u_t^* = log(\epsilon_{x,t}^2)$. Observe that ε_t and u_t^* are not correlated.

The resulting state-space representation is linear but not Gaussian since the measurement error u_t^* is distributed as a $\ln(\chi_1^2)$. We approximate $\ln(\chi_1^2)$ using a mixture of normals and transform the system into a Gaussian one following Kim et al. (1998). Express the distribution of u_t^* as:

$$f(u_t^*) = \sum_{k=1}^{K} q_k f_N(u_t^* | \iota_t = k),$$

where ι_t is the indicator variable selecting which member of the mixture of normals has to be used at time t. The function $f_N(\cdot)$ denotes the pdf of a normal distribution, and $q_k = Pr(\iota_t = k)$. Kim et al. (1998) select a mixture of seven normals ($K = 7$) with component probabilities q_k, means $m_k - 1.2704$, and variances r_k^2.

Table A-1: Approximating constants: $\{q_k, m_k, r_k\}$

ι	$q_k = Pr(\iota = k)$	m_k	r_k^2
1	0.00730	-10.12999	5.79596
2	0.10556	-3.97281	2.61369
3	0.00002	-8.56686	5.17950
4	0.04395	2.77786	0.16735
5	0.34001	0.61942	0.64009
6	0.24566	1.79518	0.34023
7	0.25750	-1.08819	1.26261

Conditional on $\iota_{1:T}$, the system has an approximate linear and Gaussian state-space form to which the standard Kalman filtering algorithm and the backward recursion of Carter and Kohn (1994) can be applied. Drawing h^T is, then, straightforward. The parameters associated

with h^T can be generated from the following posterior distributions:

$$\begin{aligned}\rho_h &\sim \mathcal{N}(V_{\rho_h}^{-1}(\bar{V}_{\rho_h}\bar{\rho}_h + \sigma_h^{-2}h'_{1:T-1}h_{2:T}), V_{\rho_h}^{-1}) \\ \sigma_h^2 &\sim \mathcal{IG}(\frac{\bar{T}_h + T}{2}, \bar{v}_h + d_h^2)\end{aligned}$$

where $V_{\rho_h} = \bar{V}_{\rho_h} + \sigma_h^{-2}h'_{1:T-1}h_{1:T-1}$ and $d_h^2 = (h_{2:T} - \rho_h h_{1:T})'(h_{2:T} - \rho_h h_{1:T})$.

The final task is to draw a new sample of indicators, $\iota_{1:T}$ conditional on u_t^* and h_t:

$$Pr(\iota_t = k|u_t^*, h_t) \propto q_k f_N(u_{jt}^*|2h_t + m_k - 1.2704, r_k^2).$$

B Estimation of the Extended Dynamic Factor Model

A bloc is indexed by j (where $j \in \{1, ..., J\}$), and multiple empirical indicators, denoted by $i \in \{1, ..., N\}$, exhibit a shared dynamic behavior described by the function $f_t^{(j)}$:

$$\begin{aligned}
&y_{i,t}^{(j)} = a_{i,t}^{(j)} + b_{i,t}^{(j)} f_t^{(j)} + u_{i,t}^{(j)}, \\
&a_{i,t}^{(j)} = a_{i,0}^{(j)} + a_{i,1}^{(j)} t, \\
&f_t^{(j)} = \phi_{f,1}^{(j)} f_{t-1}^{(j)} + ... + \phi_{f,p}^{(j)} f_{t-p}^{(j)} + \sigma_{f,t}^{(j)} \epsilon_{f,t}^{(j)}, \quad \epsilon_{f,t}^{(j)} \sim \mathcal{N}(0,1), \\
&b_{i,t}^{(j)} = b_{i,t-1}^{(j)} + \sigma_{b_i}^{(j)} \epsilon_{b_i,t}^{(j)}, \quad \epsilon_{b_i,t}^{(j)} \sim \mathcal{N}(0,1), \\
&u_{i,t}^{(j)} = \phi_{u_i,1}^{(j)} u_{i,t-1}^{(j)} + ... + \phi_{u_i,q}^{(j)} u_{i,t-q}^{(j)} + \sigma_{u_i,t}^{(j)} \epsilon_{u_i,t}^{(j)}, \quad \epsilon_{u_i,t}^{(j)} \sim \mathcal{N}(0,1), \\
&h_{k,t}^{(j)} = h_{k,t-1}^{(j)} + \sigma_{h_k}^{(j)} \epsilon_{h_k,t}^{(j)}, \quad \sigma_{k,t}^{(j)} = \sigma_k^{(j)} \exp(h_{k,t}^{(j)}), \quad \epsilon_{h_k,t}^{(j)} \sim \mathcal{N}(0,1), \quad k \in \{f, u_1, ..., u_N\}.
\end{aligned} \tag{A-13}$$

Variables without the superscript j signify that they are generated globally or derived from cross-bloc averages.

We assume that the global factor is expressed as weighted averages of the local factors through the following equations:

$$\begin{aligned}
&y_{i,t} = a_{i,t} + b_{i,t}\left(\sum_{j=1}^{J} w_j f_t^{(j)}\right) + u_{i,t}, \\
&a_{i,t} = a_{i,0} + a_{i,1} t, \\
&b_{i,t} = b_{i,t-1} + \sigma_{b_i} \epsilon_{b_i,t}, \quad \epsilon_{b_i,t} \sim \mathcal{N}(0,1), \\
&u_{i,t} = \phi_{u_i,1} u_{i,t-1} + ... + \phi_{u_i,q} u_{i,t-q} + \sigma_{u_i,t} \epsilon_{u_i,t}, \quad \epsilon_{u_i,t} \sim \mathcal{N}(0,1), \\
&h_{k,t} = h_{k,t-1} + \sigma_{h_k} \epsilon_{h_k,t}, \quad \sigma_{k,t} = \sigma_k \exp(h_{k,t}), \quad \epsilon_{h_k,t} \sim \mathcal{N}(0,1), \quad k \in \{f, u_1, ..., u_N\}.
\end{aligned} \tag{A-14}$$

For ease of exposition, we partition the model unknowns into:

$$\Theta_{f-}^{(j)} = \{\phi_f^{(j)}, \sigma_f^{(j)}, h_f^{(j),T}\}, \quad \Theta_b^{(j)} = \{b^{(j),T}, \sigma_b^{(j)}\}, \quad \Theta_u^{(j)} = \{a_0^{(j)}, a_1^{(j)}, \phi_u^{(j)}, \sigma_u^{(j)}, h_u^{(j),T}\},$$

where $j \in \{1, ..., J\}$ indexes a bloc and

$$\Theta_{f+} = \{f^{(1),T}, ..., f^{(J),T}\}, \quad \Theta_w = \{w_1, ..., w_J\}, \quad \Theta_b = \{b^T, \sigma_b\}, \quad \Theta_u = \{a_0, a_1, \phi_u, \sigma_u, h_u^T\}.$$

In total, the model unknowns are summarized as follows

$$\Theta = \left\{\Theta_{f+}, \Theta_w, \Theta_b, \Theta_u, \{\Theta_{f-}^{(j)}, \Theta_b^{(j)}, \Theta_u^{(j)}\}_{j=1}^J\right\}. \tag{A-15}$$

B.1 Modified Gibbs sampler

We adapt the Gibbs sampler to estimate the model unknowns Θ as follows. Without loss of generality, let's assume that we are at the k-th iteration:

(M1) Update $\left[\{\Theta_{f-}^{(j)}, \Theta_b^{(j)}, \Theta_u^{(j)}\}_{j=1}^J\right]^{(k+1)}$ conditional on $\Theta_{f+}^{(k)}, \Theta_w^{(k)}, \Theta_b^{(k)}, \Theta_u^{(k)}$: For each bloc $j \in \{1, ..., J\}$, we iterate through (G1), (G2), and (G3), as summarized in Appendix A.1.

(M2) Update $\Theta_b^{(k+1)}$ and $\Theta_u^{(k+1)}$ conditional on $\left[\{\Theta_{f-}^{(j)}, \Theta_b^{(j)}, \Theta_u^{(j)}\}_{j=1}^J\right]^{(k+1)}$, $\Theta_{f+}^{(k)}$, and $\Theta_w^{(k)}$: We iterate through (G2), and (G3), as summarized in Appendix A.1. At this step, when we condition on the set of local factors, the parameters and states governing local dynamics $\left[\{\Theta_{f-}^{(j)}, \Theta_b^{(j)}, \Theta_u^{(j)}\}_{j=1}^J\right]^{(k+1)}$ do not impact the update of global parameters.

(M3) Update $\Theta_{f+}^{(k+1)}$ conditional on $, \Theta_w^{(k)}, \Theta_b^{(k+1)}, \Theta_u^{(k+1)}$ and $\left[\{\Theta_{f-}^{(j)}, \Theta_b^{(j)}, \Theta_u^{(j)}\}_{j=1}^J\right]^{(k+1)}$. Appendix B.2 provides the detailed instruction.

(M4) Update $\Theta_w^{(k+1)}$ conditional on $\Theta_{f+}^{(k+1)}, \Theta_b^{(k+1)}, \Theta_u^{(k+1)}$ and $\left[\{\Theta_{f-}^{(j)}, \Theta_b^{(j)}, \Theta_u^{(j)}\}_{j=1}^J\right]^{(k+1)}$. Appendix B.3 provides the detailed instruction.

B.2 Drawing the local factors

We re-express (A-13) as:

$$\begin{aligned}
\tilde{y}_{i,t}^{(j)} &= \tilde{a}_{i,t}^{(j)} + \tilde{b}_{i,t}^{(j)} \tilde{f}_t^{(j)} + \sigma_{u_i,t}^{(j)} \epsilon_{u_i,t}^{(j)}, \\
\tilde{y}_{i,t}^{(j)} &= (y_{i,t}^{(j)} - \phi_{u_i,1}^{(j)} y_{i,t-1}^{(j)} ... - \phi_{u_i,q}^{(j)} y_{i,t-q}^{(j)}), \\
\tilde{a}_{i,t}^{(j)} &= a_{i,0}^{(j)}(1 - \phi_{u_i,1}^{(j)} ... - \phi_{u_i,q}^{(j)}) + a_{i,1}^{(j)}(t - \phi_{u_i,1}^{(j)}(t-1) ... - \phi_{u_i,q}^{(j)}(t-q)), \\
\tilde{b}_{i,t}^{(j)} &= \begin{bmatrix} b_{i,t}^{(j)} & -b_{i,t-1}^{(j)} \phi_{u_i,1}^{(j)} & \dots & -b_{i,t-q}^{(j)} \phi_{u_i,q}^{(j)} \end{bmatrix}.
\end{aligned} \tag{A-16}$$

Note that (A-16) implies the following state-space representation:

$$\begin{bmatrix} \tilde{y}_{1,t}^{(j)} \\ \vdots \\ \tilde{y}_{N,t}^{(j)} \end{bmatrix} = \begin{bmatrix} \tilde{a}_{1,t}^{(j)} \\ \vdots \\ \tilde{a}_{N,t}^{(j)} \end{bmatrix} + \begin{bmatrix} \tilde{b}_{1,t}^{(j)} \\ \vdots \\ \tilde{b}_{N,t}^{(j)} \end{bmatrix} \cdot \begin{bmatrix} f_t^{(j)} \\ f_{t-1}^{(j)} \\ \vdots \\ f_{t-q}^{(j)} \end{bmatrix} + \begin{bmatrix} \sigma_{u_1,t}^{(j)} \epsilon_{u_1,t}^{(j)} \\ \vdots \\ \sigma_{u_N,t}^{(j)} \epsilon_{u_N,t}^{(j)} \end{bmatrix},$$
$$\begin{bmatrix} f_t^{(j)} \\ f_{t-1}^{(j)} \\ \vdots \\ f_{t-q}^{(j)} \end{bmatrix} = \begin{bmatrix} \phi_{f,1}^{(j)} & \dots & \phi_{f,p}^{(j)} & \dots \\ 1 & \dots & 0 & \dots \\ 0 & \ddots & \vdots & \dots \\ \dots & 0 & 1 & \dots \end{bmatrix} \begin{bmatrix} f_{t-1}^{(j)} \\ f_{t-2}^{(j)} \\ \vdots \\ f_{t-q-1}^{(j)} \end{bmatrix} + \begin{bmatrix} \sigma_{f,t}^{(j)} \epsilon_{f,t}^{(j)} \\ 0 \\ \vdots \\ 0 \end{bmatrix}. \tag{A-17}$$

For ease of illustration, we re-express the state-space representation in (A-17) as

$$\begin{aligned} \tilde{\mathbf{y}}_t^{(j)} &= \tilde{\mathbf{a}}_t^{(j)} + \tilde{\mathbf{b}}_t^{(j)} \mathbf{f}_t^{(j)} + \boldsymbol{\sigma}_{u,t}^{(j)} \odot \boldsymbol{\epsilon}_{u,t}^{(j)}, \\ \mathbf{f}_t^{(j)} &= \boldsymbol{\phi}_f^{(j)} \mathbf{f}_{t-1}^{(j)} + \boldsymbol{\sigma}_{f,t}^{(j)} \odot \boldsymbol{\epsilon}_{f,t}^{(j)}. \end{aligned} \tag{A-18}$$

The measurement equation of (A-14) can be expressed similarly as:

$$\tilde{\mathbf{y}}_t = \tilde{\mathbf{a}}_t + \tilde{\mathbf{b}}_t \left(\sum_{j=1}^{J} w_j \mathbf{f}_t^{(j)} \right) + \boldsymbol{\sigma}_{u,t} \odot \boldsymbol{\epsilon}_{u,t}. \tag{A-19}$$

We concatenate (A-18) and (A-19) in:

$$\begin{bmatrix} \tilde{\mathbf{y}}_t \\ \tilde{\mathbf{y}}_t^{(1)} \\ \vdots \\ \tilde{\mathbf{y}}_t^{(J)} \end{bmatrix} = \begin{bmatrix} \tilde{\mathbf{a}}_t \\ \tilde{\mathbf{a}}_t^{(1)} \\ \vdots \\ \tilde{\mathbf{a}}_t^{(J)} \end{bmatrix} + \begin{bmatrix} w_1 \tilde{\mathbf{b}}_t & w_2 \tilde{\mathbf{b}}_t & \dots & w_J \tilde{\mathbf{b}}_t \\ \tilde{\mathbf{b}}_t^{(1)} & \mathbf{0} & \dots & \mathbf{0} \\ \vdots & \vdots & \ddots & \vdots \\ \mathbf{0} & \mathbf{0} & \dots & \tilde{\mathbf{b}}_t^{(J)} \end{bmatrix} \begin{bmatrix} \mathbf{f}_t^{(1)} \\ \vdots \\ \mathbf{f}_t^{(J)} \end{bmatrix} + \begin{bmatrix} \boldsymbol{\sigma}_{u,t} \odot \boldsymbol{\epsilon}_{u,t} \\ \boldsymbol{\sigma}_{u,t}^{(1)} \odot \boldsymbol{\epsilon}_{u,t}^{(1)} \\ \vdots \\ \boldsymbol{\sigma}_{u,t}^{(J)} \odot \boldsymbol{\epsilon}_{u,t}^{(J)} \end{bmatrix},$$
$$\begin{bmatrix} \mathbf{f}_t^{(1)} \\ \vdots \\ \mathbf{f}_t^{(J)} \end{bmatrix} = \begin{bmatrix} \boldsymbol{\phi}_f^{(1)} & \dots & \mathbf{0} \\ \vdots & \ddots & \vdots \\ \mathbf{0} & \dots & \boldsymbol{\phi}_f^{(J)} \end{bmatrix} \begin{bmatrix} \mathbf{f}_{t-1}^{(1)} \\ \vdots \\ \mathbf{f}_{t-1}^{(J)} \end{bmatrix} + \begin{bmatrix} \boldsymbol{\sigma}_{f,t}^{(1)} \odot \boldsymbol{\epsilon}_{f,t}^{(1)} \\ \vdots \\ \boldsymbol{\sigma}_{f,t}^{(J)} \odot \boldsymbol{\epsilon}_{f,t}^{(J)} \end{bmatrix}. \tag{A-20}$$

Based on the state-space representation in (A-20), we draw $[\ \mathbf{f}_t^{(1)'} \ \dots \ \mathbf{f}_t^{(J)'}\ ]$ for all $t \in \{1, ..., T\}$, i.e., Θ_{f+}, based on the forward filtering and backward smoothing algorithm explained in Appendix A.5.

B.3 Drawing the weights associated with the local factors

We re-arrange (A-19) as follows:

$$\tilde{\mathbf{y}}_t - \tilde{\mathbf{a}}_t = \begin{bmatrix} \tilde{\mathbf{b}}_t \mathbf{f}_t^{(1)} & \tilde{\mathbf{b}}_t \mathbf{f}_t^{(2)} & \dots & \tilde{\mathbf{b}}_t \mathbf{f}_t^{(J)} \end{bmatrix} \begin{bmatrix} w_1 \\ w_2 \\ \vdots \\ w_J \end{bmatrix} + \boldsymbol{\sigma}_{u,t} \odot \boldsymbol{\epsilon}_{u,t}. \tag{A-21}$$

By defining:

$$\begin{aligned} \widehat{\mathbf{y}}_t &\equiv \left(\tilde{\mathbf{y}}_t - \tilde{\mathbf{a}}_t\right) \oslash \boldsymbol{\sigma}_{u,t} \\ \widehat{\mathbf{x}}_t &\equiv \begin{bmatrix} \tilde{\mathbf{b}}_t \mathbf{f}_t^{(1)} \oslash \boldsymbol{\sigma}_{u,t} & \tilde{\mathbf{b}}_t \mathbf{f}_t^{(2)} \oslash \boldsymbol{\sigma}_{u,t} & \dots & \tilde{\mathbf{b}}_t \mathbf{f}_t^{(J)} \oslash \boldsymbol{\sigma}_{u,t} \end{bmatrix} \end{aligned}$$

where $A \oslash B$ means A is divided by B element-wise, we can re-express (A-21) as

$$\widehat{\mathbf{y}}_t = \widehat{\mathbf{x}}_t \mathbf{w} + \boldsymbol{\epsilon}_{u,t}. \tag{A-22}$$

We refer to Appendix A.6 for drawing $\mathbf{w}$.

C Data

C.1 Geopolitical fragmentation indicators

Descriptions and data sources are found below.

1. **The trade openness ratio**
   Description. The trade openness ratio is defined as the sum of exports and imports of goods and services divided by nominal GDP. The global indicator is constructed as the sum of all countries' exports and imports divided by world nominal GDP in current U.S.$. The definition is isomorphic to a country's trade openness weighted by the nominal GDP share. The bloc indicators are calculated accordingly for a group of countries in each bloc.
   Frequency. Quarterly.
   Sources. Exports and imports are obtained from the balance of payment (BoP) statistics in the International Financial Statistics (IFS). GDP is also taken from the IFS, and missing values are imputed by the linear interpolation of the annual GDP series in the World Economic Outlook (WEO) Database. Since Chinese trade data have a limited period (since 2005:Q1) in the IFS, they are imputed by trade partners' exports and imports available in the IMF Direction of Trade Statistics.

2. **The FDI ratio**

   Description. The foreign direct investment (FDI) ratio is the sum of FDI inflows and outflows in the BoP statistics divided by nominal GDP. The global and bloc indicators are constructed in the same way as the trade openness ratio.

   Frequency. Quarterly.

   Sources. The IFS and WEO database. The same as the trade openness ratio.

3. **The financial flow ratio**

   Description. The financial flow ratio is calculated as the sum of inflows and outflows associated with portfolio investment and other investments in the BoP statistics as a share of nominal GDP. The global indicator and bloc indicators are constructed in the same way as the trade openness ratio.

   Frequency. Quarterly.

   Sources. The IFS and WEO database. The same as the trade openness ratio.

4. **The migration flow ratio**

   Description. Migration flows are defined as the absolute number of net migration flows in each country as a share of the population. The global and bloc indicators are calculated as the weighted average of a respective group of countries using population weights.

   Frequency. Annual.

   Sources. Data are obtained from the World Population Prospects 2022 by the United Nations.

5. **The patent flows**

   Description. Cross-border patents are those filed in one country by a resident of another. Patent data are from International Patent and Citations across Sectors (INPACT-S) compiled by LaBelle et al. (2023). The database is based on PATSTAT Global Autumn 2021—a commonly used patent dataset—but LaBelle et al. (2023) impute missing data using available information and recover a large number of observations. The global and bloc indicators are calculated as the sum of a respective group of countries.

   Frequency. Annual.

   Sources. Data are obtained from INPACT-S compiled by LaBelle et al. (2023).

6. **The number of trade restrictions**

   Description. The Global Trade Alert (GTA) compiles a government statement that includes a credible announcement of a meaningful and unilateral change in the relative treatment of foreign versus domestic commercial interests. The foreign commercial interests considered by the GTA are trade in goods and services, investment, and labor force migration. All documented changes reflect unilateral government action and thus

exclude changes coordinated within bilateral trade agreements or the multilateral trading system. We count the number of announcements made (with equal weights), since the information regarding the magnitude of their economic impacts is not available. Bloc indicators are the sum of the announcements made by countries in each bloc.
Frequency. Monthly data are converted to quarterly series.
Source. Data are obtained from the Global Trade Alert.

7. **The capital control measure**
Description. We follow Fernández et al. (2016) for the definition of capital control measures. The IMF's Annual Report on Exchange Arrangements and Exchange Restrictions (AREAER) reports the presence of rules and regulations for international transactions by asset categories for each country. Fernández et al. (2016) use the narrative description in the AREAER to determine whether there are restrictions on international transactions, with 1 representing the presence of a restriction and 0 representing no restriction according to several rules. For instance, if the narrative of control involves "authorization," "approval," "permission," or "clearance," from a public institution, the control is deemed to be in place, while it is not if a requirement is "reporting," "registration," or "notification." A quantity restriction on investment (e.g., "ceiling") is regarded as a control. Also, if restrictions are imposed on sectors that are not deemed to have a macroeconomic effect or are associated with a particular country or small group of countries for non-macroeconomic reasons, they are not categorized as capital controls. They construct 1 or 0 indicators in each country for inflows and outflows of 10 asset categories (equity, bonds, money market instruments, collective investment, financial credits, foreign direct investment, derivatives, commercial credits, financial guarantees, and real estate). Then, a country indicator is calculated as the average of the 20 sub-indicators. The global and bloc indicators are calculated as the weighted average of a respective group of countries using PPP GDP weights.
Frequency. Annual.
Sources. Fernández et al. (2016). The extended series, updated on August 12, 2021, is available at the website. PPP GDP is obtained from the WEO Database.

8. **The number of sanctions**
Description. The number of sanctions is taken from the Global Sanctions Data Base (GSDB) constructed by Felbermayr et al. (2020). The GSDB defines sanctions as binding restrictive measures applied by individual nations, country groups, the United Nations (UN), and other international organizations to address different types of violations of international norms by inducing target countries to change their behavior or to constrain their actions. Sanctions often substitute military force, and the database focuses on effective sanctions while excluding threats. The GSDB classifies sanctions

by type into five categories covering trade (e.g., export/import ban), financial activity (e.g., freezing a bank account), arms (e.g., restrictions on arms sales), military assistance (e.g., prohibiting monetary or personal assistance), and travel (e.g., travel ban), plus a residual category collecting other sanctions. If a sanction spans multiple categories, it is regarded as one action. The database version 3, published in June 2023, includes 1,325 sanctions that were enforced over the 1949-2023 period. The global indicator is the total number of sanctions in place at each time point. The bloc indicators are the sum of those imposed by countries in the bloc or imposed on them. When a sanction is implemented by a group of countries or an international organization, it is counted in a bloc if at least one country joins the sanction. For instance, a sanction imposed by the UN is counted in each of the U.S.-EU, CHN-RUS, and Others blocs.

Frequency. Annual.

Source. Felbermayr et al. (2020). The extended series is available on the website.

9. **The geopolitical risk index**

Description. The geopolitical risk (GPR) index provides a news-based measure of adverse geopolitical events and associated risks. It is constructed by counting the number of articles related to adverse geopolitical events in each newspaper each month as a share of the total number of news articles. The search is organized into eight categories: War Threats, Peace Threats, Military Buildups, Nuclear Threats, Terror Threats, Beginning of War, Escalation of War, and Terror Acts. We use the historical index, which started in 1900 and is based on three major newspapers in the U.S.: the Chicago Tribune, the New York Times, and the Washington Post. The bloc indicators are the weighted average of country-specific indices for each bloc with PPP GDP weights. Country-specific indices are constructed by counting the monthly share of all newspaper articles that both (1) meet the criterion for inclusion in the GPR index and (2) mention the name of the country or its major cities. They are available for 44 different advanced and emerging countries. The resulting indices capture the U.S. perspective on risks posed by, or involving, the country in question.

Frequency. Monthly data are converted to quarterly series.

Source. Caldara and Iacoviello (2022). The extended series is available on the website. PPP GDP is obtained from the WEO Database.

10. **The trade policy uncertainty**

Description. The trade policy uncertainty (TPU) index is based on the frequency of joint occurrences of trade policy and uncertainty terms across major newspapers.[1] It covers seven newspapers: Boston Globe, Chicago Tribune, Guardian, Los Angeles

[1] Caldara et al. (2020) constructed indicators from 3 sources: newspaper coverage, firms' earnings calls, and tariff rates. We use the one based on newspaper coverage, which was updated in recent months.

Times, New York Times, Wall Street Journal, and Washington Post. The index is calculated by counting the monthly frequency of articles discussing trade policy uncertainty (as a share of the total number of news articles) for each newspaper. The index is then normalized to 0 for a 1% article share. No country-specific or bloc indicators are available.

Frequency. Monthly data are converted to quarterly series.

Source. Caldara et al. (2020). The extended series is available on the website.

11. **The energy-related uncertainty index**

Description. The energy-related uncertainty index (EUI) is constructed by text analysis of the monthly country report of the Economist Intelligence Unit for 28 developed and developing countries. An economic uncertainty index is constructed for each country following the approach in the World Uncertainty Index by Ahir et al. (2022), i.e., by counting the frequency of terms such as "uncertainty" as a share of total words in the same report. Then, the same approach is taken to calculate an energy-related index from the same source by focusing on keywords, including "energy," "oil," "OPEC," and "climate change." A global index is a simple average of countries' indices or weighted by GDP. We use the GDP-weighted index. As country-specific series are not published, we cannot create bloc indices.

Frequency. Monthly data are converted to quarterly series.

Source. Dang et al. (2023). The series is downloaded from the website.

12. **The migration fear index**

Description. The Migration Fear Index is constructed by counting the number of newspaper articles with at least one term related to migration (e.g., "border control") and fear (e.g., "fear," "concern"), and then dividing by the total count of newspaper articles. The index is available for four countries: the UK, Germany, France, and the U.S. The global index is a simple average of these countries' standardized indices.

Frequency. Monthly data are converted to quarterly series.

Source. Bloom et al. (2015). The series is downloaded from the website.

13. **The number of international conflicts**

Description. In the Uppsala Conflict Data Program (UCDP) database, armed conflicts are incidences of the use of armed force by an organized actor against another organized actor or against civilians that result in at least one direct death. International conflicts are defined as armed conflicts across states or internationalized intra-state conflicts. As the UCDP database records the start and end of each conflict, we calculate the global indicator by counting the number of international conflicts in place each month. Bloc indicators are not constructed because the incidences of conflicts are concentrated in the Others bloc and the U.S.-EU and the China-Russia blocs do not show meaningful

dynamics.

Frequency. Monthly data are converted to quarterly series.

Source. The data are taken from the UCDP Onset Dataset version 23.1 available on the website.

14. **The UN General Assembly Kappa Score**

Description. The measure represents similarities in voting patterns in the United Nations General Assembly. Compared to a simple measure of the sum of the squared actual deviation between their votes (scaled by the sum of the squared maximum possible deviations between their votes), the kappa score corrects the observed variability of the countries' bilateral voting outcomes with the variability of each country's voting outcomes around its own average outcome and the difference between the two countries' average outcomes. The global indicator is the simple average of all country pairs. Bloc indicators are calculated as the simple average score of each bloc's countries.

Frequency. Annual.

Source. The data are downloaded from the database built by Häge (2017).

C.2 Sample countries

Table A-2: List of countries for the LP

Category	Countries
AEs (34 countries)	Australia, Austria, Belgium, Canada, Switzerland, Cyprus, Czech, Germany, Denmark, Spain, Estonia, Finland, France, U.K., Greece, Hong Kong, Ireland, Israel, Italy, Japan, South Korea, Lithuania, Luxembourg, Latvia, Malta, Netherlands, Norway, New Zealand, Portugal, Singapore, Slovakia, Slovenia, Sweden, U.S.
EMs (27 countries)	Argentina, Bulgaria, Brazil, Chile, Colombia, Costa Rica, Ecuador, Croatia, Hungary, India, Indonesia, Jamaica, Jordan, Kazakhstan, Mexico, North Macedonia, Philippines, Poland, Romania, Russia, Saudi Arabia, El Salvador, Serbia, Thailand, Turkey, Ukraine, South Africa

Notes: Country classification of AEs and EMs follows the IMF WEO. Underlined countries have data available for the panel VAR analysis.

C.3 Narrative episodes: Reflecting on geopolitical fragmentation

Table A-3: Fragmentation and globalization episodes

	Period	Event	Descriptions	Impact (1 for fragmentation and -1 for globalization)
1	1988:Q4	First state sovereignty in the USSR	On November 16, 1988, Estonia was the first Soviet republic to declare state sovereignty. The event is often characterized as a trigger of the dissolution of the USSR.	-1
2	1989:Q4	Fall of the Berlin Wall	On November 9, 1989, following a press conference led by Günter Schabowski, the party leader in East Berlin and the top government spokesman, East Germans began gathering at the Berlin Wall and finally let the checkpoints open.	-1
3	1990:Q1	First independence from the USSR	On March 11, 1990, Lithuania became the first republic that declared full independence restored from the Soviet Union. This was followed by other republics' independence.	-1
4	1990:Q3	Iraqi invasion of Kuwait	On August 2, Iraq launched an invasion of Kuwait. After defeating Kuwait on August 4, Iraq went on to militarily occupy the country.	1
5	1991:Q1	Gulf War	On January 16, 1991, the U.S.-led multinational coalition started an aerial bombing campaign. The attack followed the no response by Iraq to the UNSC Resolution 678, adopted on November 29, 1990, and due by January 15, 1991, that required Iraq to withdraw from Kuwait.	1
6	1991:Q3	USSR 1991 August coup	During August 19-22, 1991, top military and civilian officials of the USSR attempted a coup to seize control of the country from Mikhail Gorbachev. Though the coup failed, it reduced the power of Gorbachev's regime and accelerated the resolution of the USSR.	-1
7	1991:Q4	Dissolution of the USSR	On December 8, 1991, Boris Yeltsin, Leonid Kravchuk, and Stanislav Shushkevich—the leaders of Russia, Ukraine, and Belarus—signed the Belovezha Accords, which declared that the Soviet Union had ceased to exist and established the Commonwealth of Independent States (CIS).	-1
8	1994:Q1	NAFTA implementation	On January 1, 1994, the North American Free Trade Agreement (NAFTA) came into force among the U.S., Canada, and Mexico, superseding the 1988 Canada-U.S. FTA.	-1
9	1994:Q2	NATO intervention in Serbia	On April 10, 1994, NATO launched an air support mission bombing several Serb targets at the request of UN commanders, followed by the increases in NATO involvement in Bosnia.	1

Table A-4: Fragmentation and globalization episodes (cont.)

	Period	Event	Descriptions	Impact (1 for fragmentation and -1 for globalization)
10	1995:Q1	WTO formation / Mercosur implementation	On January 1, 1995, the World Trade Organization (WTO) commenced operations, replacing the General Agreement on Tariffs and Trade (GATT). As of January 1, 1995, Mercosur, a South American trade area, became a customs union with common external tariffs.	-1
11	1999:Q1	Introduction of the Euro	On January 1, 1999, the euro was introduced in non-physical form, with the exchange rate with participating countries' currencies based on the market rates on December 31, 1998.	-1
12	1999:Q1	NATO intervention in Kosovo	On March 24, 1999, NATO started the bombing campaign against Yugoslavia during the Kosovo War.	-1
13	2001:Q3	9.11	On September 11, 2001, coordinated Islamist suicide terrorist attacks were carried out by Al-Qaeda against the U.S.	1
14	2003:Q1	Iraq War	On March 20, 2003, the U.S., joined by the UK, Australia, and Poland, launched a bombing campaign, followed by a ground invasion of Iraq.	1
15	2010:Q4	Arab Spring	Protests in Tunisia escalated after the self-immolation of Tunisian Mohamed Bouazizi on December 17, 2010, which led to a democratization in Tunisia (Jasmine Revolution) and spread across the Arab world (Arab Spring).	1
16	2014:Q3	U.S. attack on ISIL	On August 8, 2014, the U.S. began airstrikes against the Islamic State of Iraq and the Levant (ISIL) in Iraq. This followed the declaration by the group to rename itself as an Islamic State and a worldwide caliphate on June 29, 2014.	1
17	2016:Q2	Brexit vote	On June 23, 2016, the "Brexit" referendum, which asked the electorate whether the country should remain a member of, or leave, the European Union (EU), took place in the UK. The referendum resulted in favor of leaving the EU, triggering the process of the country's withdrawal from the EU (Brexit).	1
18	2017:Q4	Breakup of ISIL	On October 17, 2017, the Syrian Democratic Forces announced the full capture of Raqqa in Syria, the de facto capital city of ISIL. In December 2017, it was reported that ISIL had lost all strategic territory in Iraq.	-1

Table A-5: Fragmentation and globalization episodes (cont.)

	Period	Event	Descriptions	Impact (1 for fragmentation and -1 for globalization)
19	2018:Q2	U.S.-China trade war (phases 1-3)	On July 6, 2018, U.S. tariffs on $34 billion of Chinese goods (announced on June 16) came into effect (phase 1). On August 23, tariffs of 25% on additional Chinese products worth $16 billion (announced on August 8) became effective (phase 2). On September 24, a 10% tariff on $200 billion worth of Chinese goods began (announced on September 17) (phase 3).	1
20	2019:Q2	U.S.-China trade war (increase in phase 3)	On May 10, 2019, the U.S. raised the tariff on phase 3 products from 10% to 25% (announced on May 5).	1
21	2019:Q3	U.S.-China trade war (phase 4)	On September 1, 2019, the U.S. imposed new 15% tariffs on about $112 billion of Chinese products.	1
22	2022:Q1	Russian invasion of Ukraine	On February 24, 2022, Russia invaded Ukraine. The invasion became the largest attack on a European country since World War II.	1

C.4 Country classification and indicators for local indices

Three geopolitical blocs are considered: the U.S. and EU countries bloc (U.S.-EU), China and Russia bloc (CHN-RUS), and the remaining countries bloc (Others). EU countries are the member states of the European Union each period. The union republics of the Union of Soviet Socialist Republics (USSR) are included in the CHN-RUS bloc before its dissolution in 1991Q4. Countries are listed in Table A-6. Empirical fragmentation indicators for individual blocs are presented in Figure A-1.

Table A-6: List of countries in each bloc

Category	Countries
U.S.-EU bloc	U.S., Belgium, France, Germany, Italy, Luxembourg, Netherlands (founders); Denmark, Ireland (1973Q1-); Greece (1981Q1-); Spain (1986Q1-); Austria, Finland, Sweden (1995Q1-); Portugal (1996Q1-); Cyprus, Czechia, Estonia, Hungary, Latvia, Lithuania, Malta, Poland, Slovakia, Slovenia (2004Q2-); Bulgaria, Romania (2007Q1-); Croatia (2013Q3-); UK (-2019Q4)
CHN-RUS bloc	China, Russia, Ukrainian SSR (Ukraine), Byelorussian SSR (Belarus), Uzbek SSR (Uzbekistan), Kazakh SSR (Kazakhstan), Georgian SSR (Georgia), Azerbaijan SSR (Azerbaijan), Lithuanian SSR (Lithuania), Moldavian SSR (Moldova), Latvian SSR (Latvia), Kirghiz SSR (Kyrgyz), Tajik SSR (Tajikistan), Armenian SSR (Armenia), Turkmen SSR (Turkmenistan), Estonian SSR (Estonia) (-1991Q4)
Others bloc	All other countries

Figure A-1: Bloc indicators

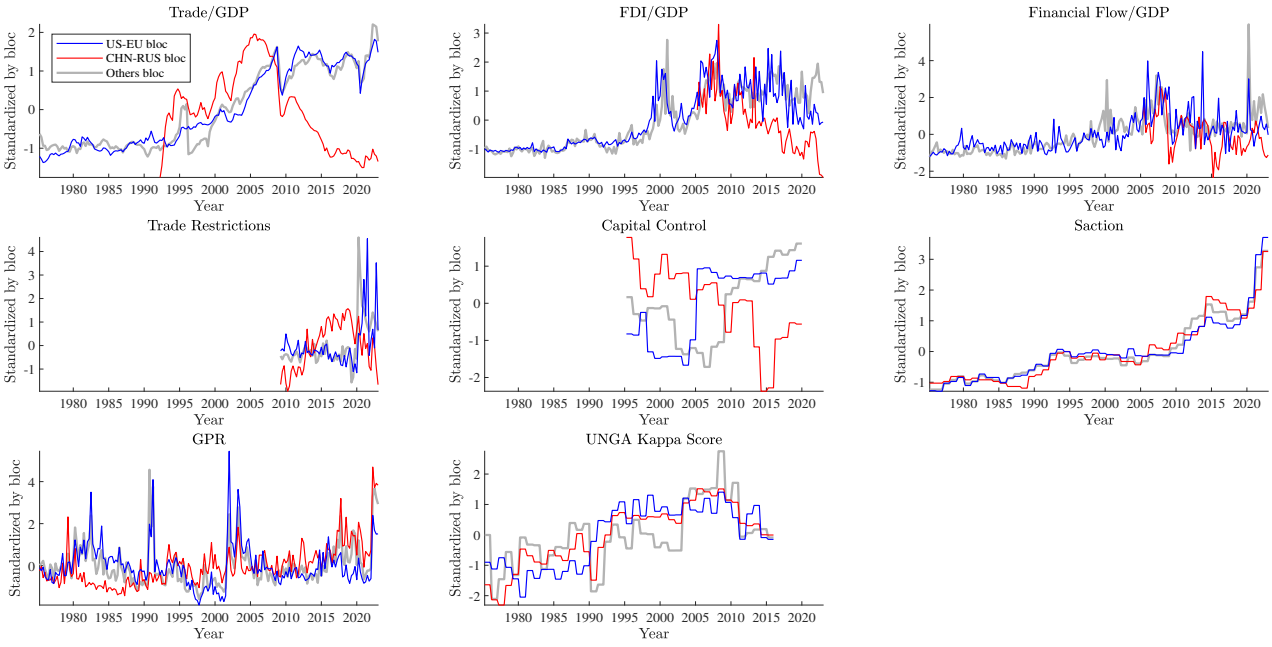

D Supplementary Figures and Tables

D.1 Posterior estimates

Figure A-2: Posterior estimates: Constants, persistence, volatilities

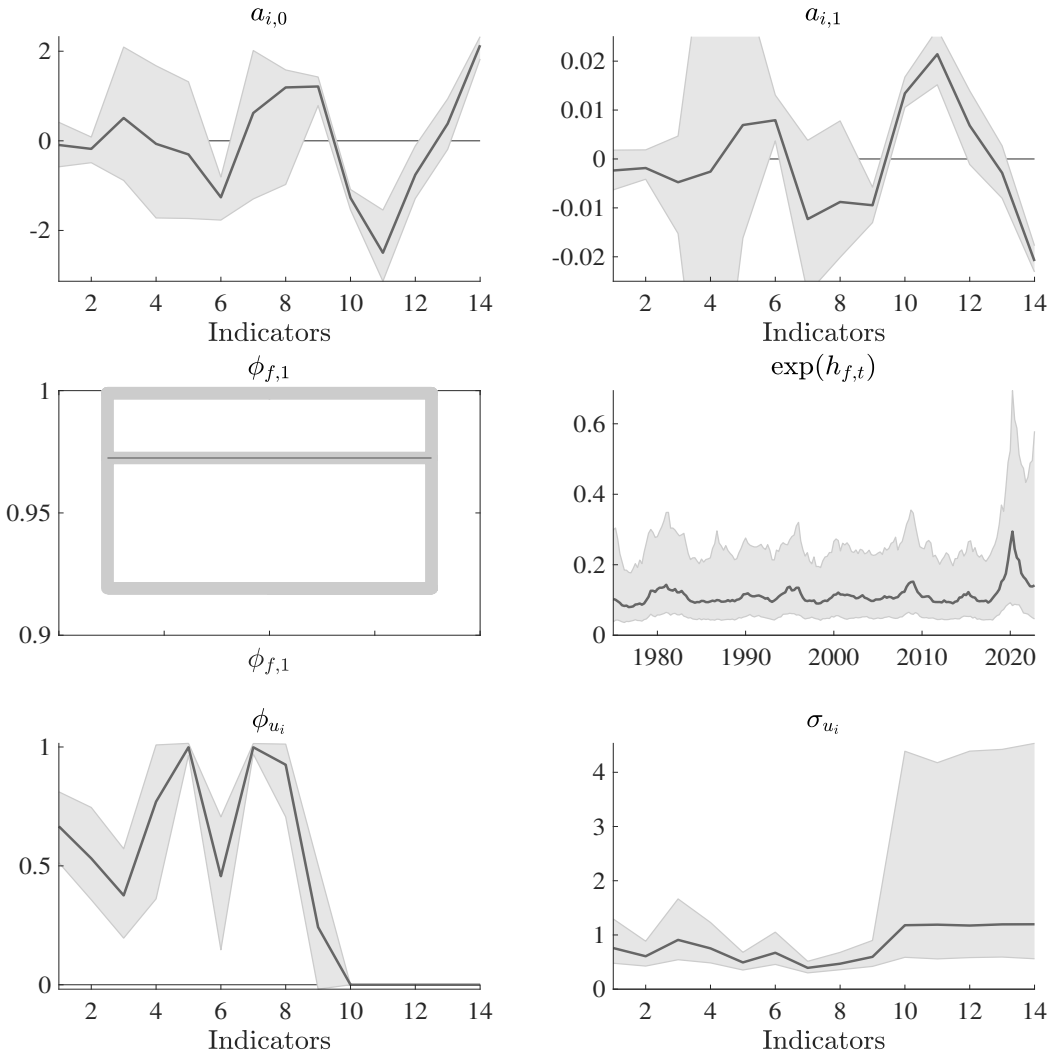

Notes: Posterior median estimates accompanied by 90% credible intervals. The numerical assignment for each indicator aligns with the sequential order in which the indicators are displayed in Panel (A) of Figure 1.

Figure A-3: Posterior estimates: Factor loadings and volatilities for idiosyncratic error terms

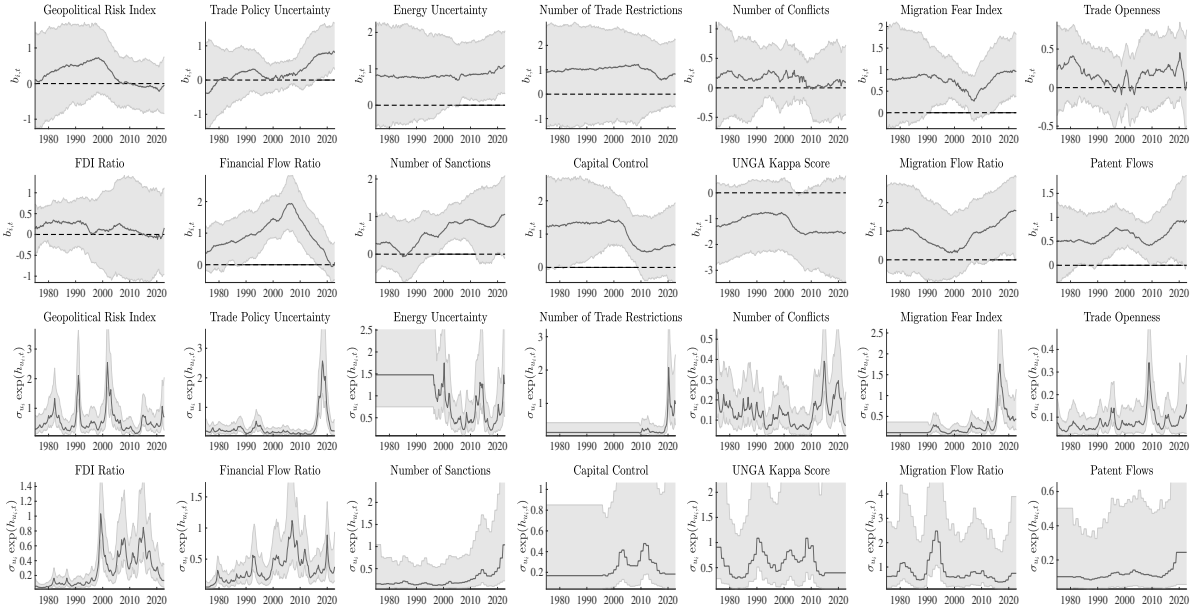

Notes: Posterior median estimates accompanied by 90% credible intervals.

D.2 Descriptive statistics

Table A-7: Descriptive statistics of countries

Variable	N. of observations	Mean	Median	Std. Dev.	10th percentile	90th percentile
All countries						
GDP per capita (1,000 PPP$)	5,837	32.1	30.4	19.2	10.6	53.5
GDP growth per capita (%)	5,958	2.2	2.3	5.3	-3.0	7.7
Exports share (% of GDP)	6,019	48.3	37.3	38.2	19.3	83.2
Imports share (% of GDP)	6,019	47.9	37.5	34.4	20.4	79.6
Trade share (% of GDP)	6,019	96.2	74.6	72.2	40.1	161.2
Currency peg (1 for peg)	6,025	0.25	0	0.43	0	1
AEs						
GDP per capita (1,000 PPP$)	3,583	42.4	40.2	17.0	26.1	58.8
GDP growth per capita (%)	3,735	2.1	2.1	4.7	-2.5	7.1
Exports share (% of GDP)	3,765	56.2	40.4	44.9	20.4	122.2
Imports share (% of GDP)	3,765	53.6	38.7	40.3	21.1	114.3
Trade share (% of GDP)	3,765	109.9	79.9	85.1	41.9	240.1
Currency peg (1 for peg)	3,765	0.22	0	0.41	0	1
EMs						
GDP per capita (1,000 PPP$)	2,254	15.8	14.5	7.6	8.2	25.0
GDP growth per capita (%)	2,223	2.4	3.0	6.1	-3.8	8.3
Exports share (% of GDP)	2,254	34.9	32.1	15.3	18.1	54.3
Imports share (% of GDP)	2,254	38.3	34.6	17.3	19.0	65.0
Trade share (% of GDP)	2,254	73.2	67.7	31.3	37.5	118.7
Currency peg (1 for peg)	2,260	0.30	0	0.46	0	1

Notes: Pooled sample during 1986 to 2019. Currency peg is an indicator variable that takes zero for the floating exchange rate regime and one otherwise, according to the IMF Annual Report on Exchange Arrangements and Exchange Restrictions (AREAER).

D.3 Robustness checks

D.3.1 Alternative selection of indicators: Replicating the SVAR results

Figure A-4: Sensitivity to the choice of indicators in factor estimation

(A) Core 7 indicators (Trade Openness, FDI, Financial flows, Sanctions, GRI, TPU, Conflicts)

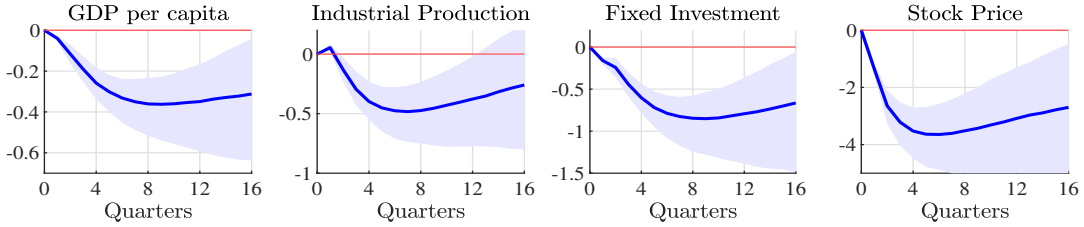

(B) All indicators in (A) & Trade Restrictions & Migration Fear Index

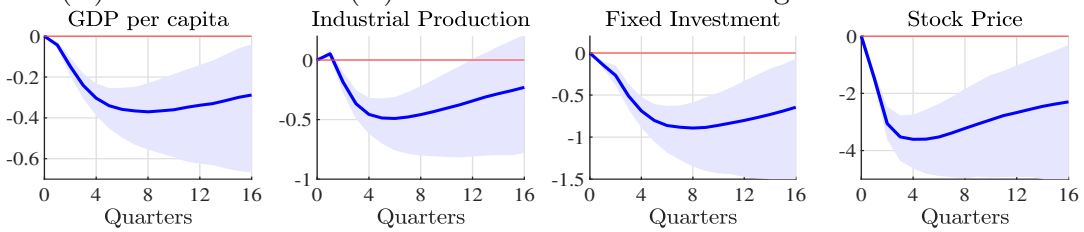

(C) All indicators in (B) & Energy Uncertainty

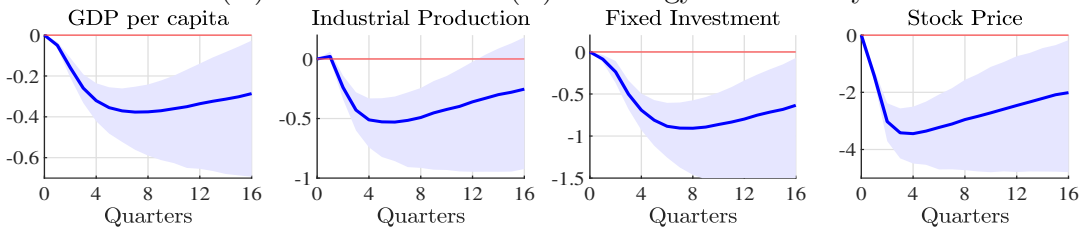

(D) All indicators in (B) & Capital Control

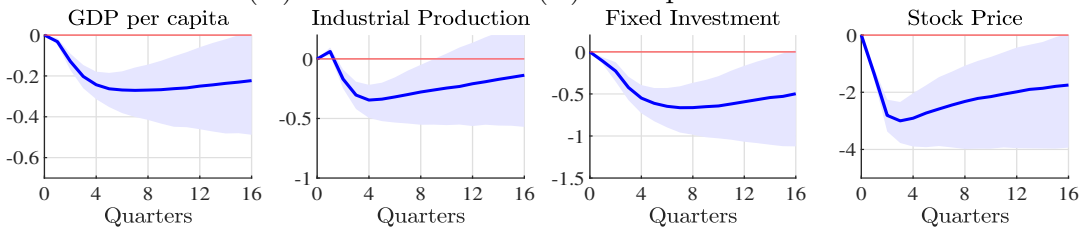

(E) All indicators in (B) & Energy Uncertainty & Capital Control

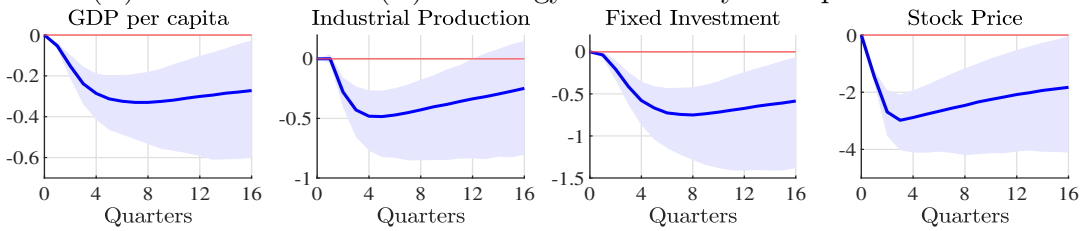

Notes: Sample of AEs and EMs. Percent responses to a one-standard-deviation shock to the factor. Shaded areas indicate the 90th percentile. The Core 7 indicators are available on a quarterly basis throughout the entire sample period.

D.3.2 Alternative prior choices: Replicating the SVAR results

Figure A-5: Sensitivity to the prior specification of factor estimation

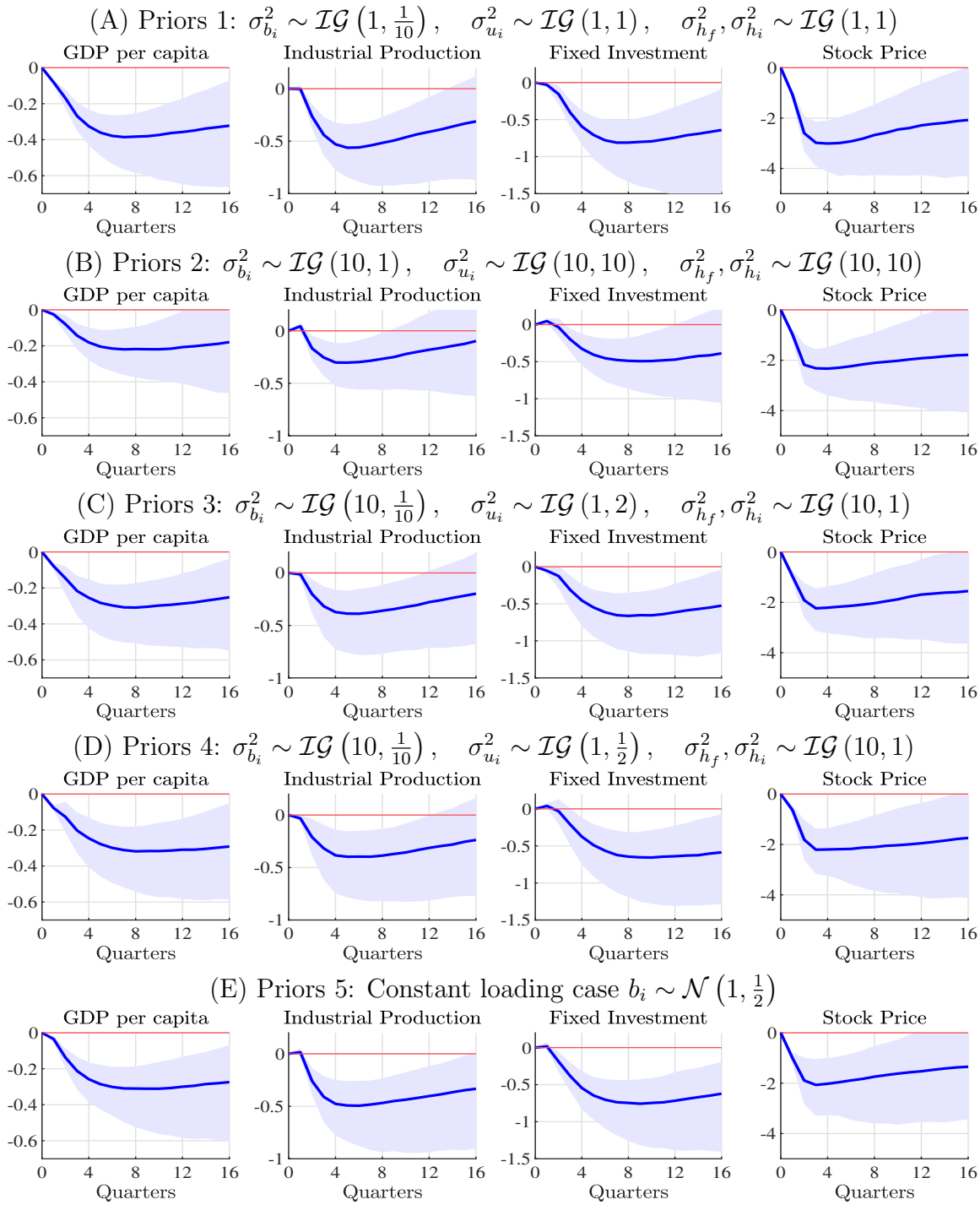

Notes: Sample of AEs and EMs. Percent responses to a one-standard-deviation shock to the factor. Shaded areas indicate the 90th percentile. Unless specified otherwise, we adhere to the previously discussed priors for the remaining parameters.

D.3.3 Using Trade Openness instead: Replicating the SVAR results

Figure A-6: Sensitivity to replacing the fragmentation index with Trade Openness

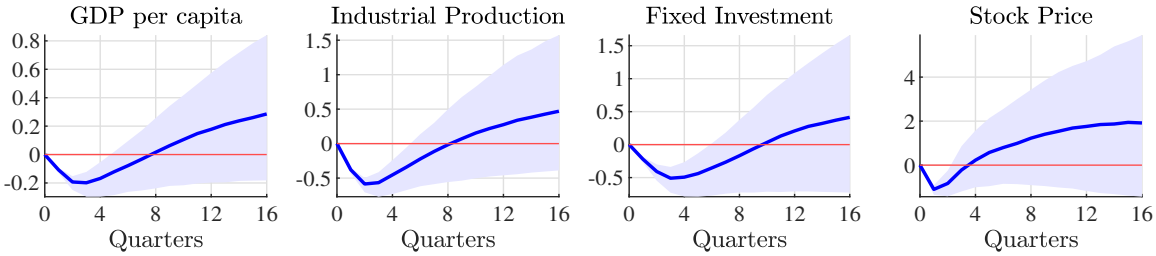

Notes: The fragmentation index is replaced with the trade share in the SVAR. Sample of AEs and EMs. Percent responses to a one-standard-deviation shock to each indicator. The sign of the responses is flipped. Shaded areas indicate the 90th percentile.

D.3.4 Alternative Cholesky ordering: Replicating the SVAR results

Figure A-7: SVAR with different Cholesky ordering

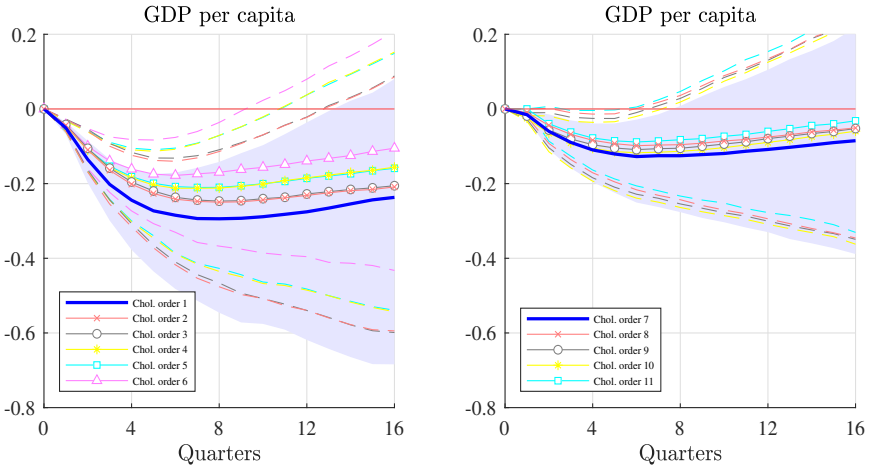

Notes: Sample of AEs and EMs. Percent responses to a one-standard-deviation fragmentation shock. Different lines display the IRFs in which the fragmentation index is ordered in the i-th place in the Cholesky decomposition. The ordering of other variables is kept unchanged. Shaded areas and dashed lines indicate the 90th percentiles where standard errors are clustered by time.

D.3.5 Alternative identification schemes: Replicating the LP results

Figure A-8: Sensitivity to alternative identification schemes

(A) Identified through differencing

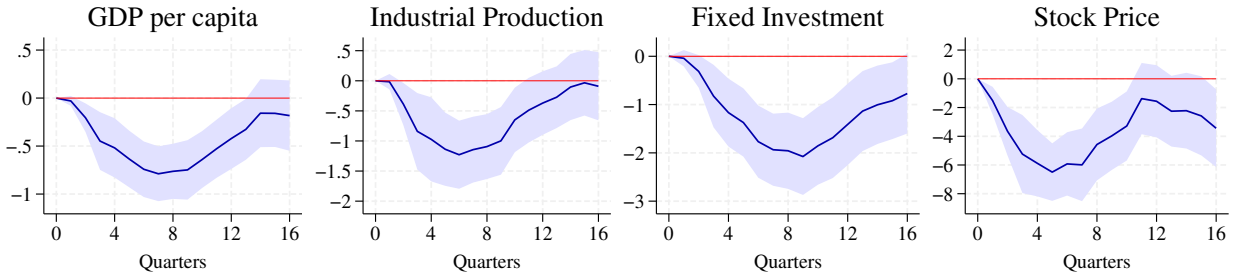

(B) Identified through Cholesky decomposition

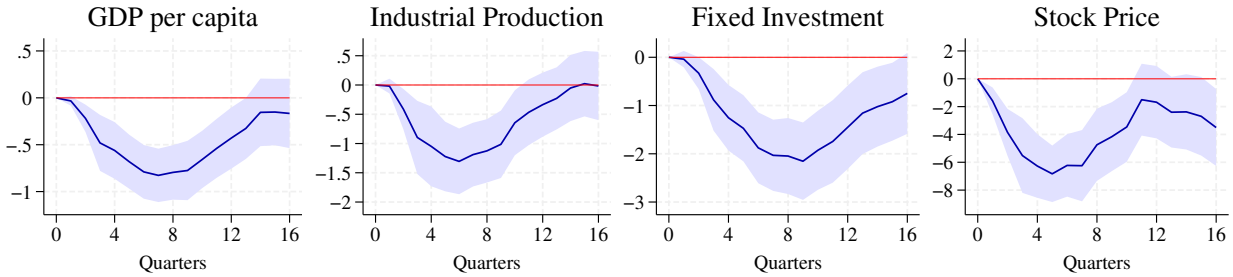

Notes: Sample of AEs and EMs. Percent responses to a one-standard-deviation shock to the factor. Shaded areas indicate the 90th percentile. In Panel (A), the first difference of the factor is used as a shock. In Panel (B), a global VAR with the first seven variables of the baseline panel VAR is run with the sample period of 1986:Q2 to 2022Q4, and the fragmentation shock is identified through the Cholesky decomposition.

D.3.6 Local and global fragmentation shocks: SVAR

Figure A-9: IRFs to local and global fragmentation shocks in local economies

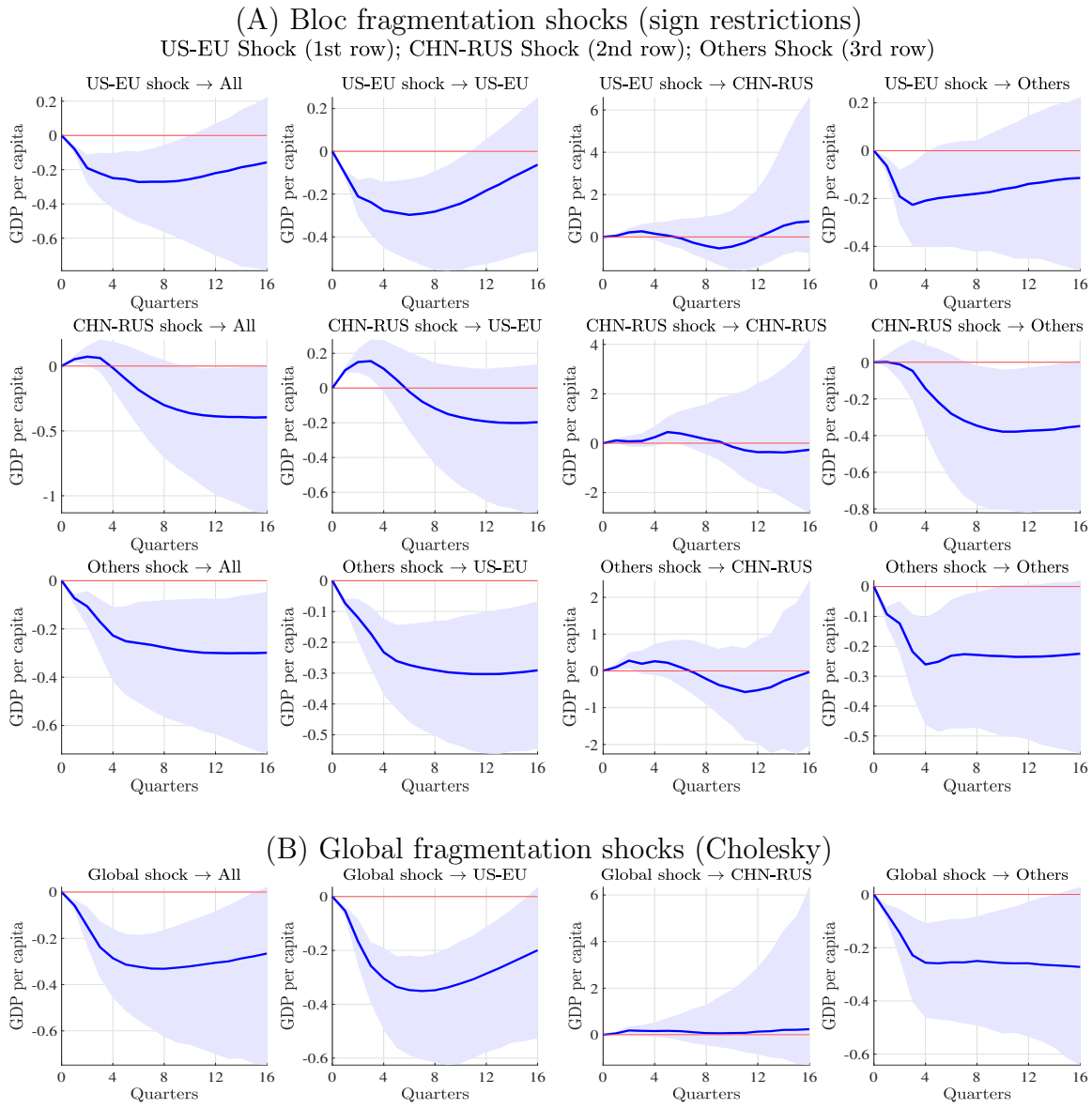

Notes: Percent responses to a one-standard-deviation shock. Shaded areas indicate the 90th percentiles where standard errors are clustered by time. The first columns correspond to the baseline analysis in which all countries are included in a panel VAR. In Panel (A), the horizon of sign restrictions is set to 4 quarters.